

RAIN FOLLOWS THE FOREST: LAND USE POLICY, CLIMATE CHANGE, AND ADAPTATION*

Florian Grosset, Anna Papp, and Charles A. Taylor[†]

December 2023

Abstract

Human actions can alter the regional climate, particularly via land use. We analyze the Great Plains Shelterbelt, a large-scale forestation program in the 1930s across the US Midwest. This program led to a decades-long increase in precipitation and decrease in temperature. Changes extended to adjacent unforested land up to 200km away—enabling us to directly study climate adaptation. In downwind places facing improved growing conditions, farmers expanded corn acreage and switched to more water-intensive production. This paper highlights the endogeneity of the climate to land use changes, and the potential for tree planting to regionally mitigate climate change impacts.

*This paper greatly benefited from comments by Francis Annan, Douglas Almond, Eyal Frank, Robert Heilmayer, Rick Hornbeck, Solomon Hsiang, Kyle Meng, Wolfram Schlenker, Jeffrey Shrader, Aaron Smith, Marco Tabellini, Andrew Wilson, Brian Wright, and participants at the NBER EEE Summer Institute, World Bank-GWU-UVA Economics of Sustainable Development Conference, LSE Environment Week, CEEP-Federal Reserve Bank of New York Environmental Economics and Policy Conference, Occasional Workshop in Environmental and Resource Economics (UCSB), Stanford GSB Climate Conference, Simon Agriculture & Natural Resource Seminar (UC Berkeley and UC Davis), AERE Summer Conference, Northeast Workshop on Energy Policy and Environmental Economics, Seminar in Planetary Management, and Sustainable Development Colloquium. Aidan McCullen and Yixian Liu provided excellent research assistance. We are grateful to Dr Meagan Snow for sharing digitized Shelterbelt data. All errors and omissions are our own.

[†]Grosset: Columbia University (f.grosset@columbia.edu); Papp: Columbia University (Corresponding author. Email: ap3907@columbia.edu); Taylor: Harvard University (ctaylor@hks.harvard.edu).

1 Introduction

The popularity of large-scale tree planting has grown rapidly over the last two decades. Prominent examples include the Great Green Wall, a pan-African initiative to grow trees across the entire continent along the Sahel, and the One Trillion Trees Initiative launched by the World Economic Forum in 2020. In lower-income countries like China, Pakistan, and Mexico, the goal of these programs is to mitigate erosion, dust storms, and landslides. In higher-income settings, the focus is increasingly on carbon sequestration, bolstered by recent work arguing that afforestation¹ and forest restoration could sequester enough carbon to reduce atmospheric CO₂ levels by 25% (Bastin et al. 2019).²

As a natural and proven way to capture and store carbon, tree planting is popular among policy makers.³ A recent study on pathways to net zero emissions estimated that \$900 billion must be invested by 2030 into afforestation, requiring 160 million hectares of new forest land globally (McKinsey Global Institute 2022)—an area larger than France, Spain, and Germany combined.

The natural science literature proposes another potential outcome of large-scale tree planting: local climate change. Such climate effects are driven by trees' impact on energy and water fluxes. Atmospheric models predict an increase in precipitation where trees are planted, as well as in downwind areas (Bonan 2008).⁴ Such policy-induced climate change can, in turn, affect economic outcomes—both locally where the trees are planted and in locations downwind. The total effect will depend on the mechanical response to the change in climate (e.g., higher crop yields in response to more favorable growing conditions) as well as the extent to which agents adapt by adjusting their behavior in response to the new climate. Neighboring areas may also be influenced through general equilibrium effects.

In this paper, we examine the causal impact of a large-scale tree-planting program on both climate and economic outcomes. We empirically test the predictions from atmospheric models in response to afforestation and estimate the resulting magnitudes. We then leverage

¹ Afforestation involves tree planting to establish forests on land not previously forested.

² One provocative study argues that the Little Ice Age was partially driven by CO₂ declines from reforestation in the Americas following the mass death of indigenous peoples after European contact (Koch et al. 2019).

³ Over half of the 193 Paris Agreement signatory countries are prioritizing land use and forestry to achieve their CO₂ mitigation targets (UNFCCC 2022). All possible pathways identified by the IPCC to limit global warming at the 1.5° include the removal of CO₂ from the atmosphere (IPCC 2019).

⁴ For temperature, the net local effect is ambiguous and depends on land characteristics. Since trees are generally darker than the land they are planted on (e.g., cropland or pasture), tree planting can decrease albedo and surface reflection, thus raising temperatures. On the other hand, trees increase evapotranspiration, which reduces temperatures. A large body of work has investigated the local and regional climate impacts of deforestation, particularly in the Amazon (Spracklen and Garcia-Carreras 2015), generally finding that deforestation reduces precipitation.

this policy-induced change to identify the long-term effects of climate change on economic outcomes and assess the extent of adaptation.

We focus on the Great Plains Shelterbelt in the United States. Planned in response to the Dust Bowl, the government-funded program aimed to reduce soil erosion and dust storms in the US Midwest. Announced in 1932 and implemented from 1935 to 1942, the program led to the planting of 220 million trees. Trees were grown in windbreaks, which consisted of numerous strips of trees planted between fields and farms. The resulting ‘belt’ of trees bisected the US from north to south, spanning 1,700km and crossing six states from North Dakota to Texas.

The largest afforestation effort of its time, the Great Plains Shelterbelt is now rivaled in scope by multiple tree-planting projects around the world. We focus on this specific program to leverage its unique characteristics. While it was implemented over 80 years ago, we note that the socioeconomic conditions of the US Midwest in the 1940s are comparable to the many lower and middle-income countries where similar programs are being designed and implemented today. The historical context provides the long time frame required for a direct study of the drivers and consequences of climate change, i.e., changes in the *distribution* of weather events over the medium to long term. Historical data for the United States from the onset of the 20th century allow us to empirically consider a rich set of outcomes over a long period (for our main sample, 1930-1965) and precisely characterize the adaptation to climate change. This data availability, combined with the short and delimited implementation period, enables us to use simple and clean identification strategies.

We implement a difference-in-differences identification strategy that exploits prevailing wind patterns, which are the primary physical mechanism by which trees planted in a given location affect climate in nearby areas where the program is not implemented. We construct a wind exposure measure based on large-scale prevailing summer winds to approximate a given location’s exposure to winds arriving from areas afforested under the Shelterbelt. We then use variation in this continuous wind measure to compare the evolution in outcomes between areas that are, on average, more exposed to summer winds from afforested areas, to areas that are less exposed.

In a first step, we show that large-scale tree planting substantially changes the climate. To ease the interpretation of our effects, we compare counties in the 75th percentile of exposure to summer winds blowing through the Shelterbelt afforested areas to those in the 25th percentile. We find that precipitation increased by 2.0%, or 1.6mm per month, during the summer months ($p < 0.001$), and maximum temperature decreased by 0.6% (-0.10°C , $p < 0.001$)

as well. Extreme heat, which has a strong negative impact on yields, decreased even more dramatically, with degree days above 29°C falling 6.7% ($p < 0.001$) in counties more exposed to winds from the Shelterbelt. Similar effects are estimated on the Palmer Drought Severity Index (PDSI), a measure of crop water availability jointly determined by temperature and precipitation anomalies. The direction of these effects is consistent with the qualitative predictions from atmospheric models. Importantly, they are not limited to areas where trees are planted: we find similar effects of exposure to winds blowing through the Shelterbelt in areas neighboring but outside the Shelterbelt.

Our results are robust to a range of sensitivity tests, designed to address, among others, potential concerns with endogeneity or mean reversion. Results hold using i) an instrumental variable approach to account for the potential strategic selection of farmers into the Shelterbelt project; ii) a long differences method to account for uncertainty about the specific timing of treatment; iii) binary treatment variables (separating Shelterbelt, downwind neighbor, and other neighbor groups) instead of the continuous wind exposure measure; and iv) a synthetic difference-in-differences method to account for potential differential pre-trends (including potential differential exposure to the Dust Bowl that could induce differential mean-reversion). We further conduct placebo tests using non-downwind neighboring counties, where we do not expect the Shelterbelt would alter the climate. Point estimates for these areas are an order of magnitude smaller, and statistically indistinguishable from zero. These tests, along with other robustness checks, indicate that these potential concerns are unlikely to be confounding our estimates.

Having established that the Shelterbelt project induces climate change, our second step involves estimating the effects of this climate change on the economy and testing for any follow-on adaptation. We limit our analysis to counties near, but not directly afforested under the Shelterbelt project, to isolate the effect of climate change from other changes potentially associated with Shelterbelt participation. We focus on agriculture, a sector highly exposed to climate and representative a large share of the economy of the post-war US Midwest.

We find that crop production increased significantly in response to this policy-induced change in climate among counties downwind from the Shelterbelt. This increase in production was driven by the expansion in corn acreage rather than increased productivity: area of corn harvested increased by 35% ($p < 0.001$) in counties in the 75th percentile of wind exposure compared to counties in the 25th percentile, while there was a smaller and less precise increase in yields of 3% ($p = 0.111$). Furthermore, farmers reallocated production from pasture to cropland and switched from less water-sensitive crops (e.g., wheat) to more water-sensitive crops (e.g., corn). Results hold after implementing the same set of robustness checks used

to confirm the climate effects.

Interestingly, the net effect on corn yields is of similar magnitude to what would be predicted in response to short-term climate shocks using the canonical model of Schlenker and Roberts (2009). This implies that most of the longer-term adaptation to the more favorable climate regime occurred along the extensive margin through corn expansion and water-intensive crop switching—rather than through increasing yields. This aligns with the intuition that the expansion of cropland occurs along a frontier of lower-yielding marginal lands (Olmstead and Rhode 2002), which are brought into production due to the marginal change in climate.

Our study advances our understanding of the interactions between climate and the economy both substantively and methodologically. First, we contribute to an emerging literature on the endogeneity of local climate to land use. Economists generally assume local climate to be exogenous to local socioeconomic activities. We provide novel evidence that this is not the case.⁵ Other recent work in this vein includes Braun and Schlenker (2023), who find that the historical expansion of irrigation in the US affected temperature, both locally and in downwind areas. In the Amazonian context, Araujo (2023) finds a downwind precipitation response to changes in forest cover and then models the responses of farmers in terms of land use and agricultural productivity. Taken together, these recent working papers confirm the external validity of the endogeneity of climate to land use changes in a range of settings, and the potential follow-on socioeconomic impacts. But neither papers map to an explicit policy choice contemplated by governments around the world in response to climate change: large-scale tree planting.

Our findings have implications for our understanding of place-based policies involving localized changes in productivity. Such changes are known to induce economic spillovers to other regions through the spatial reallocation of capital and labor (Kline and Moretti 2014; Bustos et al. 2016; Bustos et al. 2020; Asher et al. 2022; Hornbeck and Moretti 2023). Our study, which shows that land use policy can induce climate change across an area far beyond where the policy is implemented, demonstrates economic spillovers through a third potential channel involving climate change.

We next describe the methodological implications that extend from our findings on climate

⁵This idea has long been explored in the natural science literature. Atmospheric models are used to describe the response of local and regional climate to changes in land use (Devaraju et al. 2015). Other studies estimate the reduced-form climate effect of various land use changes, including irrigation (e.g., Lobell et al. 2008; DeAngelis et al. 2010; Mueller et al. 2016; Braun and Schlenker 2023), crop choice (Loarie et al. 2011; Georgescu et al. 2011), and forestation (Smith et al. 2023; Alkama and Cescatti 2016; Peng et al. 2014). Many of these studies are either observational or compare trends in areas with land use change to adjacent unchanged areas, and, therefore, cannot identify spillover effects.

endogeneity. The elasticity of agricultural productivity with respect to climate is a key parameter to assessing the economic consequences of climate change, including agricultural outcomes, food security, structural transformation, and trade flows. As detailed below, we propose a new reduced-form approach to estimating this elasticity using a policy-induced change in the long-run climate to measure productivity effects inclusive of adaptive responses. This resulting elasticity comprises both the direct, mechanical effect of weather shocks drawn from a different distribution (i.e., climate change), combined with the effects of adaptation.

In terms of the direct impact of climate change, our findings have implications for the vast body of work using climate as a source of identifying variation. While debates on the economic effects of climate can be traced back centuries (Montesquieu 1750), the credibility revolution in economics and growing concerns about anthropogenic climate change have spurred a revival of studies focusing on climate impacts. A wide range of outcomes are affected by annual weather shocks (see Dell et al. 2012 for a seminal paper, and for reviews Dell et al. 2014 and Carleton and Hsiang 2016). However, identifying the effects of climate (i.e., the distribution of weather events over time) based on observed variations in the realizations of that distribution (i.e., weather shocks) presents challenges (Hsiang 2016; Kolstad and Moore 2020; Lemoine 2021).⁶

One approach to assessing adaptation involves accounting for how responses to climate shocks vary across space by average climate (Butler and Huybers 2013; Heutel et al. 2021; Auffhammer 2022; Hultgren et al. 2022), the idea being that if the same extreme heat event causes less deaths in a warm climate than a cold climate, that difference is (partly) due to adaptation. This useful and intuitive approach still faces concerns about potential confounders across space, as well as “weather-vs-climate” issue discussed above. Another way to get at adaptation is through “long differences”: estimating the correlation between long-term changes in climate and outcomes of interest (Burke and Emerick 2016). Identification then relies on the assumption that long-term trends in climate are exogenously determined across spatial units. Our results showcase the potential for reverse causality-driven bias when using spatial variation in climate trends to assess impacts on economic outcomes—given that these climate trends themselves may be driven by endogenously-determined policies—and thereby invite increased caution when using climate trends as a source of identifying variation.

By demonstrating that local climate change can be policy induced, our study provides a natural direction to advance this literature. We can indeed use standard applied microeconomic

⁶The effect of weather shocks can be larger than climate change if adaptation is less costly over the long run than over the short run (e.g., if fixed cost investments are required). The converse is possible if short-run adaptation strategies like irrigation become more costly over time (Hornbeck and Keskin 2014).

tools, such as difference-in-differences or regression discontinuity design, to assess whether policies have the potential to affect the climate and to subsequently study the consequences of this policy-induced climate change. Importantly, exploiting such policy changes can then enable researchers to argue more convincingly for causal identification of climate effects, particularly in locations downwind or otherwise not directly affected by the policy.

In an agricultural context, existing research provides valuable insights on how economic agents respond to productivity shocks, including soil erosion from the US Dust Bowl (Hornbeck 2012) and permanent reductions in groundwater in India (Blakeslee et al. 2020). Economic agents, however, may respond differently to climate change—that we conceptualize, following Hsiang (2016), as a permanent change in the distribution of transitory productivity shocks—than to single, either permanent or transitory, productivity shocks. There is a robust body of work on US crop yield responses and adaptation to climate change with mixed results.⁷ Most of our current knowledge of mechanisms for agricultural adaptation to climate comes from observational studies.⁸

Our work relates to studies focusing on adaptation to medium-to-long-term fluctuations in the monsoon regime in India (Kala 2017; Taraz 2017; Liu et al., forthcoming). These generally combine agricultural and economic data over several decades with five to ten year changes in the timing and intensity of monsoons, as well as temperature and precipitation, to provide causal evidence on crop and labor adaptation. Our study advances this literature by providing direct causal evidence of significant farmer adaptation to a long-term change in continental climate across a range of dimensions, and estimates how these responses moderate the overall impact of climate change (relative to no adaptation). Our paper also builds on work studying the Great Plains Shelterbelt over the long term and its effect on local agriculture practices and outcomes (Li 2021; Howlader 2023).

In summary, we find that the Great Plains Shelterbelt—in part inspired by a climate shock itself—induced a significant change in regional climate. This policy-driven climate change, in turn, affected economic outcomes for decades in locations downwind from the policy itself. We also find strong evidence of climate adaptation by farmers. The geographic scale of these effects are large, encompassing an area the size of California.

Recent global enthusiasm for tree planting for climate change mitigation raises many questions about how to best design tree planting projects. There are many valid concerns around

⁷ See, for instance, Schlenker and Roberts 2009; Butler and Huybers 2013; Annan and Schlenker 2015; Burke and Emerick 2016; Malikov et al. 2020; Yu et al. 2021.

⁸ Such adaptive channels include crop choice (Kurukulasuriya and Mendelsohn 2008; Sloat et al. 2020; Cui 2020; Burlig et al. 2021), ecological practices (Schulte et al. 2017), and irrigation (Taylor 2022).

large-scale tree planting, including the scale of the land required, the timing and permanence of the CO₂ reductions, and its potential ecological impacts. We believe our study of the Great Plains Shelterbelt, which entailed a unique ecological design that we describe later, is relevant to the many countries considering large-scale tree planting projects as a way to meet their national climate mitigation targets and maximize societal benefits. This is especially true among countries still highly dependent on agriculture (like the US Midwest in the 1940s) as well as global breadbasket regions with similar soil and climate characteristics to the US Great Plains.

2 Background

The Great Plains Shelterbelt project, also known as the Prairie States Forestry Project, was a Great Depression-era effort to plant forest buffers and windbreaks in the US Midwest. It was the largest afforestation program to date, with over 220 million trees planted between 1935 and 1942. Unlike other regions historically covered by forests in which the expansion of farming came through extensive deforestation, most of the Midwest was covered in grasslands. In 1800, less than 1% of the area of future Shelterbelt counties was forested. While the problems of drought and soil erosion were not new in the prairies of the Great Plains, the destructive Dust Bowl of the 1930s led to a renewed interest in making the Great Plains states more habitable and suitable for agriculture.

Franklin D. Roosevelt conceived of the shelterbelt idea while running for President (Droze 1977). FDR had a long-running interest in forestry and experience with reforestation projects as Governor of New York and believed that an investment in forestry might improve the climate and agriculture of the Great Plains. As president, Roosevelt commissioned a report recommending the planting of trees in 100-foot strips or “shelterbelts” that protect homes, crops, and livestock from the wind and destructive dust storms. FDR’s plan, which was controversial among foresters at the time (Munns and Stoeckeler 1946), called for a Shelterbelt 100 miles across and 1,300 miles long, bisecting the continental US from North Dakota to Texas along the the country’s 18-inch rainfall line. Figure A1 shows both the planned and actual zone of Shelterbelt planting.

FDR signed an executive order in 1934, and the first tree was planted in 1935 in Oklahoma. For the most part, seedlings from nurseries were planted instead of seeds to increase survival rates, and irrigation was not used. In total, over 30 species of trees and shrubs were selected—tall and short trees, fast and slow growing trees, hardwoods and conifers—most of which were native and thus locally adapted (Read 1958) to ensure species diversity and ecological

resilience in a way that mimicked naturally-occurring forests.

At first, the government leased the land for tree planting but soon transitioned to cost-sharing programs with landowners. The Great Plains project was later part of the Works Progress Administration, which required 90% of the workers hired for the Shelterbelt project were hired from relief rolls. The program stopped in 1942 due to funding cuts that resulted from the US's World War II efforts (Droze 1977).

It is worth noting the focus of the Shelterbelt project on local and regional climate at the time of its inception. The *New York Times* described the project as an “experiment in climate control to combat the ravages of drought” when it first reported on the program (“Tree Belt in West to Fight Droughts” 1934). Indeed, Snow (2019) describes the controversy around the program as a battle between ‘ecological foresters’ who believed that policy decisions impact local climate and environmental conditions and ‘determinist geographers’ and foresters who saw climate as static.

3 Data

Our main analysis is based on a county-by-year dataset, constructed from four types of data: digitized historical maps of Shelterbelt plantings to define treatment status, wind data to construct our Shelterbelt wind exposure metric, temperature and precipitation data for our climate outcomes, and agricultural census data for our economic outcomes. We focus in our main analysis on the period 1930-1965.⁹ Our results are robust to using different start and end years.

Shelterbelt definition: We digitize maps of the Shelterbelt locations from Read (1958) for our measure of the assignment of treatment under the Shelterbelt project. Although we do not have an exact measure of trees or windbreaks planted in each county, Read (1958) maps areas with intensive afforestation. We therefore take the percentage of each county covered by “areas of concentrated Shelterbelt planting”, and define counties with over 5% of this measure (corresponding to the 20th percentile of counties with non-zero tree planting area) as Shelterbelt counties. Throughout the paper, we use “Shelterbelt counties” and “treated counties” interchangeably. Figure 1 shows the location of the concentrated Shelterbelt planting areas.

⁹ We start in 1930 due to concerns about data quality and availability before that date. We end in 1965 to limit the overlap with other agricultural changes, including the expansion of irrigation and urbanization, could be influenced by tree planting and influence the climate themselves.

We validate our Shelterbelt measure with an alternative source of data. Snow (2019) digitized the actual Shelterbelt plantings that survived during the post-treatment period from the United States Geological Survey (USGS) Topographic Map Quadrangles.¹⁰ We calculate each county's area covered by the Shelterbelts from her digitized shapefiles, and compare with our main measure. Appendix Figure A2 plots the two measures side-by-side to show the similar geographic coverage of the two measures (correlation is 0.86).

Wind data: Wind is an essential driver of regional climate change in relation to afforestation. Trees usually increase the amount of water being released into the atmosphere through evapotranspiration. This atmospheric water vapor then travels with wind, increasing precipitation in areas downwind from the tree planting. We therefore construct a measure of counties' exposure to winds from the Shelterbelt, to determine which neighbor counties are most likely to have their climate influenced by the Shelterbelt project.

For our primary analyses, we use the North American Land Assimilation System (NLDAS-2) gridded wind data available from NASA. The NLDAS-2 combines multiple sources of observations such as precipitation gauge data, satellite data, and radar precipitation measurements to produce climatological estimates with a 1/8th-degree spatial resolution.¹¹ Specifically, we use their hourly u -wind (east-west dimension) and v -wind (north-south dimension) measures, 10 meters above the surface level.

Using the NLDAS-2 data, we create a time-invariant approximate measure of how exposed each neighboring county is to winds from the shelterbelts in the summer (w_i). To do so, we project an imaginary particle at a given speed and direction, and record all counties that it crosses over the course of 24 hours. We project these particles from each vertex of each Shelterbelt county, and repeat it from each summer hour (June through August) of each year between 1981 and 2010.¹² For each particle, we use the speed and direction of the wind from NLDAS-2 for that specific origin vertex and time. To avoid a Shelterbelt county's shape from affecting the weight in our wind exposure measure, we assign each particle a weight inversely proportional to the number of vertices from their origin Shelterbelt county. In a version of the wind exposure metric, we also assign weights based on the intensity of tree

¹⁰ USGS undertook the detailed mapping of the conterminous US through the production, by hand, of over 55,000 quadrangle maps covering about 64 square miles each from 1947 to 1992. Snow 2019 identifies in each map the vegetative areas with the characteristic shape and scale of Shelterbelt plantings (e.g., linear features that run east/west or north/south) and extracts the corresponding polygons. She validates this procedure by comparing the final digitized Shelterbelt acreage totals by state to official project totals.

¹¹ NCEP North American Regional Reanalysis (NARR) data, used widely in environmental economics (e.g., Deryugina et al. 2019), is the main input for NLDAS-2 but available only 8-times a day and at a 32km grid. We use NLDAS-2 for its hourly temporal frequency and 14km spatial resolution.

¹² High-resolution wind data is only available starting in 1979. Section 5.4 addresses the potential bias that might arise from using post-treatment period wind data when classifying counties by downwind extent.

planting in the origin county. We then count, for each neighbor county, how many (weighted) particles originating from any Shelterbelt county crossed it during the simulation. Finally, we rescale the metric by dividing it by its maximum value. The resulting wind exposure metric $w_i \in [0, 1]$ is a time-invariant approximate measure of how exposed a neighbor county i is to winds from *all* Shelterbelt counties. Figure 2 illustrates the construction of the wind metric and the resulting downwind exposure for all spillover counties. Further details are provided in Appendix A.1.

Temperature and precipitation data: We construct a county-by-year panel of precipitation and temperature based on daily weather stations data, using a methodology inspired by Schlenker and Roberts (2006). We start from the Global Historical Climatology Network daily (GHCNd) dataset provided by the US National Oceanographic and Atmospheric Administration (NOAA). We clean this dataset and create a balanced panel of stations reporting between 1930 and 1965 in order to ensure that changes in the measured climate are not driven by changes in the underlying set of measuring stations. We spatially interpolate the station data to obtain a gridded dataset at a 0.1 degree resolution, and average the resulting measures at the county-by-day level. Finally, we compute for each month the average daily precipitation, average maximum temperature, maximum temperature, and total number of daily degree days at various thresholds. To move from this county-by-month dataset to county-by-year, our main analysis focus on the average of these measures over the summer months (June through August). Details on the construction of this dataset are available in Appendix A.3.

Degree days have been shown to be a relevant measure of temperature when studying impacts on crops or physiology, performing better than maximum or mean temperature, and have become widely used in economics following work by Schlenker and Roberts (2006; 2009). Yield growth increases gradually up to but decreases sharply above critical temperature thresholds. For corn, our main crop of interest, the critical threshold is 29°C, so we include 29°C degree days as one of our primary climate dependent variables.

Standard gridded weather datasets (applying complex improvements and interpolation algorithms to the raw station data) with historical coverage, such as NOAA's NCLimDiv and PRISM, do not include degree days and are at the monthly level, not allowing their computations. This motivated our choice to construct our main weather dataset directly from the daily station data. Still, we verify the robustness of our results on precipitation and mean and maximum temperature to using the standard NCLimDiv dataset.

Economic data: We use crop yields, production, and area harvested data from USDA

agricultural censuses and surveys. The National Agricultural Statistics Survey (NASS) has conducted agricultural surveys and censuses at the county level annually and every five years, respectively. For our primary specification investigating the effects of tree planting and changing climate on corn yields, we use the agricultural censuses conducted by NASS every five years. We use the digitized versions of the 1930 - 1964 censuses (8 censuses) provided by Haines et al. (2018). The main outcomes of interest are county-level corn yields, corn and wheat acreage, and acreage of land in farms and in pasture. The spatial resolution of the census data is an advantage over the agricultural survey data, which before the 1940s is available only for a subset of states and counties. Appendix Figure A11 shows the coverage of the census and surveys in our study.

4 Empirical approach

Our main empirical analyses exploit prevailing wind patterns in a difference-in-differences framework. We study changes in climate and economic outcomes not only in counties with afforestation, but also in areas near Shelterbelt counties. Tree planting may lead to precipitation in nearby *downwind* areas through the transport of the increased moisture produced from higher evapotranspiration. As wind is the primary mechanism through which afforestation leads to regional changes in climate, we use our wind exposure metric, w_i , as our primary *continuous* treatment measure. We estimate the following model

$$y_{it} = \beta(w_i \times P_t) + \gamma(\mathbf{X}_i \times Y_t) + \delta_{st} + \nu_i + \epsilon_{it} \quad (1)$$

where y_{it} is the outcome of interest at the county-year level (e.g., summer temperature, precipitation, yields), w_i is the wind exposure measure ($w_i \in [0, 1]$) described in Section 3. P_t is a dummy variable equal to one for years after 1942.¹³ We include various time-invariant controls (\mathbf{X}_i) interacted by year (Y_t) in order to account for potentially differential pretreatment characteristics that could influence crop production and yield trends. Drawn from the literature, these controls include inherent crop suitability measures from FAO GAEZ¹⁴, soil

¹³ The Shelterbelt project was conducted from 1935 to 1942. Implementation started slowly, with most trees planted in the final years of the project. (See Appendix Figure A3 for the timing.) We can further expect the impact of tree planting to increase over time, as trees grow. We therefore make the conservative choice of using 1942 as the start of the treatment period. (If treatment effects happened earlier, our estimation would underestimate the true effect.) We also implement a long differences strategy to side-step this uncertainty about the exact start of the treatment.

¹⁴ These crop suitability measures are commonly used in economics (e.g., Costinot et al. 2016). We use “low input, non-irrigation” scenario to approximate historical conditions.

characteristics¹⁵, Dust Bowl erosion measures from Hornbeck (2012), and the share of county irrigated in 1935 from the USDA agricultural census.¹⁶ We also include state-by-year (δ_{st}) and county (ζ_i) fixed effects.

Our main coefficient of interest is β , which measures the change in post-1942 outcomes for a unit increase in the wind exposure measure (w_i), equivalent to a change from no exposure to winds coming from the Shelterbelt to the maximum possible wind exposure. To aid interpretability, we multiply coefficients with the difference in wind exposure between the 25th and 75th percentile of this measure (0.21).

The effects we identify are equilibrium outcomes. For instance, it is possible that planting trees affects the downwind climate, which in turn induces people to change their land use in these downwind areas. This land use change, itself, can have a local effect on the climate. This does not threaten the internal validity of our approach: we only need to interpret the estimated coefficients as the resulting equilibrium effects of large-scale tree planting in a given area.

Our identification strategy relies on the assumptions that in the absence of tree planting, all groups of counties would have experienced the same changes in outcomes and that the group compositions do not vary over time. Assuming that group composition is not changing over time is reasonable. Indeed, as the Shelterbelt project was cut short in 1942, the tree planting did not materially continue in the region after the project's conclusion. Large-scale wind patterns also did not change—thereby keeping the wind exposure groups unchanged. The parallel trends assumption is not testable. Nonetheless, we provide evidence that the pre-treatment trends are parallel across various levels of wind exposure.

As described in Callaway et al. (2021), additional assumptions are needed to identify treated-type parameters in a difference-in-differences model with a continuous treatment variable and the interpretation of these parameters is challenging. Callaway et al. (2021) show that the coefficient from a TWFE regression such as Equation 1 can be decomposed into a weighted average of causal responses to incremental changes in treatment, if a stronger parallel trends assumption holds. This assumption requires that for all doses of treatment, the average change in outcomes over time across all units (if they had been assigned that dose) is the same average change in outcomes for units that actually receive that dose (Callaway et al. 2021). This means that there should be no selection into a particular dose. In our

¹⁵We use the share of county area covered by ustoll soils derived from USDA soil surveys. Ustolls are the more or less freely drained mollisols of subhumid to semiarid climates. Most of the ustolls on the Great Plains supported grass vegetation when the region was settled.

¹⁶While we do not directly control for irrigation in the later decades, as it may be an outcome influenced by Shelterbelts, we show that irrigation in the Ogallala region does not drive our results in Section 5.4.

setting, this is equivalent to the assumption that counties with a particular wind exposure measure w_d respond the same way, on average, to an incremental increase in wind exposure at measure w_d as all other counties with different actual wind exposure measures would (at measure w_d). This is reasonable in our setting, at least for the climate results, if an additional amount of moisture is likely to increase precipitation and lower temperature by the same amount anywhere in the region.

To address some of these challenges, we also supplement our main empirical approach with several alternative methodologies described in Section 5.3. Using these analyses, we address interpretation challenges with difference-in-differences with continuous treatment variables, the potential endogeneity of which counties are selected for the Shelterbelt project, and uncertainties in the timing of treatment effects. To address challenges in interpreting results using a continuous treatment variable, we replicate our analyses using a difference-in-differences specification with binary treatment variables for treated, downwind neighbor, other neighbor, and control counties. This methodology also allows us to run placebo checks in areas that we do not expect to be affected by afforestation. We also use an instrumental variables approach to address potential endogeneity concerns regarding the selection into taking-up tree planting under the Shelterbelt project. Finally, we also utilize a long differences approach to account for uncertainties regarding the specific timing of treatment effects.

5 Results

We now present our main results on the impact of Shelterbelt tree planting on local and regional climate, and the resulting economic consequences. We first discuss results from our difference-in-differences approach that exploits wind patterns, on climate outcomes (5.1). We then present the economic effects of this policy-induced climate change, and discuss the role of adaptation (5.2). We then show that our results are robust to a range of alternative empirical strategies (5.3), and address potential threats to the internal validity of our main results (5.4).

5.1 Climate impacts

We begin with a graph showing average climate outcomes over time (Figure 3, Panel A). For improved visibility, given the high variability of rainfall and temperature, we show three-year moving averages for precipitation and temperature measures for counties in the above and below median wind exposure. This figure allows us to visually check for the existence of

pre-exposure trends, which helps argue for the validity of the parallel trends assumptions required for identification of the difference-in-differences model. The two groups exhibit parallel trends before the treatment for the measures of precipitation and temperature.

Our regression results from our main empirical model (Equation 1) show that summer precipitation increased while summer temperature decreased in areas exposed to summer winds from the Shelterbelt. Table 1 shows the climate effect of afforestation for all regions the program affected decades after its implementation. Summer precipitation was 1.6mm higher in counties in the 75th percentile of wind exposure compared to counties in the 25th percentile of wind exposure. This is equivalent to a 2% increase relative to the average monthly summer rainfall. We also find summer temperatures decreased: average and maximum temperatures were 0.4% and 0.6% lower in areas more exposed to winds from afforested areas. Exposure to extreme temperatures harmful for corn yields also decreased significantly. Average monthly degree days above 29°C decreased by 1.9 for an increase in wind exposure from the 25th to the 75th percentile, equivalent to a 6.7% decrease relative to the mean. We find similar results when dropping directly afforested counties (Appendix Table A1). Overall, these results show that tree planting resulted in more favorable growing conditions regionally. These results are consistent with increased evapotranspiration from the Shelterbelt trees. Evaporative demand is greatest during high temperatures, which means that the cooling influence of evapotranspiration is expected to be most pronounced for periods of high temperatures (Mueller et al. 2016). This is exactly what we find, as the decreases in maximum temperatures and degree days above 29°C are greater than the decrease in average temperatures.

Temperature and precipitation jointly determine crop water availability, the variable that ultimately drives crop yields. Therefore, we also test the impact of the Shelterbelt program on an alternative proxy of crop water availability: the Palmer Drought Severity Index (PDSI).¹⁷ We observe an increase in PDSI, which represents a lower likelihood of drought conditions, in both Shelterbelt and downwind neighboring counties (Appendix Table A2).

As a robustness check, we replicate our main results without any time-invariant controls, as well as with various subsets of controls. Panel A of Figure A4 shows that our results are robust to all of these alternate specifications. We also rerun our climate results with only year fixed effects (Figure A4, Panel B), rather than state-by-year fixed effects. Next, we rerun our analyses separately dropping the project implementation years (1936 to 1942) and peak Dust Bowl years (1934, 1936, 1939) from our baseline period. Appendix Tables A3

¹⁷ PDSI measures the departure from the local average of atmospheric moisture. The index ranges from -10 to +10, with lower values signifying stronger drought conditions.

and A4 show the results are generally consistent with our main findings. Finally, to address concerns about spatial correlation, we implement Conley standard errors. We show that even using a conservative, large distance cutoff (1000km), and a range of distance cutoffs, most of our main estimates remain statistically significant despite slightly less precise estimation (Figure A6, Panel A).

5.2 Economic impacts

Our results so far show that Shelterbelt tree planting affected the regional climate, via increased summer rainfall and reduced summer temperatures. We now turn to the economic effects of this engineered change in the climate, which became more favorable to agriculture. While tree planting can have local economic consequences due to both the direct effect of afforestation and the induced change in climate, we can focus on areas *downwind* from the policy-induced tree planting, who haven't been directly affected themselves, to identify the economic consequences of a change in climate. We first estimate the effects of this changing climate on corn production, area harvested, and yields, using our difference-in-differences empirical strategy. We then test for a range of possible agricultural adaptation strategies, and quantify the relative importance of adaptation responses and direct climate effects in driving the estimated change in agricultural output.

Crop production, area harvested, and yields: As before, we begin with a graph showing crop yields over time. Note we focus on corn, a crop grown across the Midwest and for which there is extensive historical data. Panel B of Figure 3 shows annual corn production, area, and yields for all areas affected by the Shelterbelt. While there are a limited number of pre-treatment periods, there does not appear to be differential pre-trends in the 1930s.

Table 2 shows the regression results from our main empirical model (Equation 1), in regions near but not directly in the afforested Shelterbelt counties. Corn production and area harvested both increased in areas more exposed to summer winds from the Shelterbelt, but not directly afforested. Corn production was 38% higher in counties in the 75th percentile of wind exposure compared to counties in the 25th percentile of wind exposure. Similarly, corn area harvested was 35% higher in counties more exposed to winds from the afforested areas. As illustrated by Figure 5, the difference between the increase in production and area harvested is equal to the increase in yields. Since the increase in production exceeded the increase in area harvested, yields increased by 3% in counties in the 75th percentile of wind

exposure compared to counties in the 25th percentile of wind exposure.¹⁸

As with the climate results, we check robustness to excluding various and all time-invariant controls. Panel A of Figure A5 shows that the increase in production and area results are robust to all of these alternative specifications. We again rerun our results with only year fixed effects (Figure A5, Panel B), rather than state-by-year fixed effects. In Panel B of Figure A6 we show robustness of our main results to Conley standard error using various distance cutoffs.

Next, we estimate the direct (physiological) effect of the Shelterbelt-induced climate change on yields, in the downwind neighbor counties. We do so in three steps. First, we estimate the direct relationship, absent adaptation, between climate and yields. We use the canonical piece-wise linear model from Schlenker and Roberts (2009), which includes year and county fixed effects. Since identification stems from weather variations across years and counties, it does not capture farmers' response to a long-term change in the climate. We can therefore use it to compare yields under different climates in the absence of adaptation. Second, we estimate the causal effect of the Shelterbelt project on each climate variable entering the Schlenker and Roberts 2009 model, for downwind neighbor counties. We use these estimates to predict, for each county, the climate that they would have experienced absent the Shelterbelt project. Third, we use the estimated climate-yield relationship absent adaptation to predict yields both (i) under the actual realized climate and (ii) under the climate that would have existed absent the Shelterbelt project. The average difference in values from (i) and (ii) gives us the direct, physiological, effect of the Shelterbelt-induced climate change on yields.¹⁹

We calculate that corn yields in counties in the 75th percentile of the wind exposure measure increased 3.8% compared to counties in the 25th percentile from the direct (without adaptation) climate effect of the Shelterbelt tree planting. By comparison, we observe a 3.2% increase in yields in downwind neighboring counties (Figure 5). The net effect of exposure to winds from Shelterbelts is similar in magnitude to the physiological effects estimated using the canonical model of Schlenker and Roberts (2009). This implies that most of the longer-term adaptation to the more favorable climate occurred along the extensive margin through corn expansion and is consistent with the large increases we observe in the area of corn harvested.

¹⁸ While we use the agricultural censuses due to its geographical coverage and more detailed data on production and area harvested, we replicate our yield results using annual corn yield data from the NASS agricultural surveys. Figure A7 shows that we find larger increases in corn yields when using the NASS survey data. This is mainly due to differences in the geographical coverage of the datasets.

¹⁹ More details are provided in Appendix A.4.

Adaptation: We further explore whether farmers adapt to the changing climate by altering their agricultural input decisions. In other words, are farmers re-optimizing their planting decisions when the return to one output—corn, in the case of our study—increases due to the geoengineered climate change?

A first test for adaptation comes directly from the corn results. Specifically, a change in yields can be driven by a change in output, in area planted, or both. In the absence of climate adaptation, the effect of climate on yields should be entirely driven by a change in output, while the area planted should not vary. We directly test this hypothesis, with results presented in Table 2, Column (2). We can reject the hypothesis that area planted does not vary, and thereby provide evidence that farmers do adapt to the changing climate.

Next, we seek to refine our understanding of farmers' land use choice. We therefore estimate the effect of climate change on a range of potential land use choices, including cropland vs. pastureland, and planting corn vs. wheat. When crop yields increase because of more favorable growing conditions, the returns to cropland increase. If the substitution effect dominates the income effect, cropland should increase. That increase can either come by an increase in total farmland (at the cost of acquiring new land) or a decrease in pastureland (at the cost of foregoing returns from pasture). A priori, the choice will depend on the relative costs of the two options. Empirically, we find that cropland area did increase in areas more exposed to summer winds from the Shelterbelt (Column (1), Table 3), at the expense of pastureland (Column (2), Table 3), albeit the estimates are imprecise.

Corn and wheat were two of the major crops grown in the region at the time. Importantly, precipitation has historically been a major determinant of crop choice in the US. As such, dryland wheat is the main crop grown in areas with annual rainfall under 18 inches (Horner et al. 1957), while dryland corn generally requires over 25 inches annually (Neild and Newman 1987). We can therefore expect the share of cropland devoted to more water-intensive crops to increase when precipitation increases. Empirically, we see a 1.4 percentage point increase in corn's share of cropland in counties in the 75th percentile of the wind exposure measure compared to counties in the 25th percentile (Column (4), Table 3). At the same time, wheat's share of cropland decreased by 0.6 percentage points (Column (5), Table 3). In line with theory, we therefore find an increase in the share of cropland used for corn production, at the expense of wheat production.

At first, our findings could appear at odds with prior work. Li (2021) studies the local effect of the Shelterbelt project on agricultural outcomes, and finds a shift in production towards pasture. However, the author includes annual weather variables such as rainfall and

precipitation as controls, which we show are actually outcomes of the Shelterbelt.

Overall, these results point to the key role of adaptation for climate effects—and indicate that extrapolating estimates from short-term weather variations to predict climate impacts, thus omitting the potential for adaptation responses, can lead to severe bias.

5.3 Alternative specifications

In this section, we show that our results are robust to several alternative methodologies that address possible concerns with our difference-in-differences methods. These alternate results are summarized in coefficient plots in Figure 4. We next describe each of the alternative methods and corresponding results in more detail.

Instrumental variables: We address the concern that the decision to plant trees as part of the Shelterbelt project might be endogenous to changes in climate or agricultural outcomes. For instance, Howlader (2023) studies how market factors influenced Shelterbelt participation, finding that areas growing crops whose prices increased were less likely to take up tree planting. If farmers responded to these price changes by also changing other agricultural decisions that had an effect on local yields or the local climate, then our difference-in-differences estimates would be biased. For this reason, we instrument the presence of actual windbreaks with a variable related to where windbreaks were planted but unrelated to changes in climate and socioeconomic outcomes.

Specifically, similar to Li (2021), we use the zone of planned Shelterbelt planting as shown in the gray shaded area in Figure A1. This was an approximately 100-mile wide strip of land between 100° and 98° West. We treat all counties that overlap with this area as the hypothetical or planned Shelterbelt. We then repeat the wind exposure measure construction steps described in Section 3, except replace Shelterbelt counties with the planned counties. We use this planned wind exposure measure (wp_i) as an instrument for the continuous treatment variable (w_i) in our difference-in-differences model. Figure A8 shows the wind exposure instrument next to the actual wind exposure measure.

We estimate in a two-stage least squares (2SLS) regression, where the first stage is:

$$w_i = \xi_1 wp_i + \theta(\mathbf{X}_i) + \phi_s + e_i \quad (2)$$

where w_i is the wind exposure measure for each county, wp_i is the planned wind exposure measure for each county, \mathbf{X}_i is the set of time-invariant controls included in our main

specification, and ϕ_s is state fixed effects. The model for the second-stage estimation is then:

$$y_i = \beta_{IV}(w_i \times P_t) + \zeta(\mathbf{X}_i \times Y_t) + \eta_{st} + \mu_i + \epsilon_{it} \quad (3)$$

where w_i , the wind exposure measure, is instrumented by wp_i , and all other variables are as defined before.

Appendix Tables A6 shows the results of our estimation using the instrumental variables approach for climate outcomes. Column (5) shows the first stage estimation results from using the planned wind exposure metric as an instrument for actual treatment variable (Equation 2). The first stage is strong. Columns (1)-(4) of these tables show the instrumental variables estimates according to Equation 3. Our estimates for rainfall and the various temperature measures are all similar in magnitude to the main climate results presented in Table 1. We repeat the analyses for economic outcomes. Appendix Table A7 shows the results. Again, the estimates are similar in magnitude to the main corn production, area, and yield results shown in Table 2. As shown in Figure 4, these results are also robust to excluding the time-invariant controls.

Long differences: We can use a long differences approach to model changes in outcomes over time as a function of group membership (Shelterbelt, downwind neighbor, other neighbor). An advantage of utilizing a long differences method is that it is not sensitive to treatment timing. While tree planting began in 1935 and lasted throughout 1942, trees take time to grow and realize their full potential, and it is, therefore, unclear exactly when the benefits of the windbreaks began. In our difference-in-differences model, we treat years after 1942 as our post-treatment period, but we do not have to make such an assumption in our long differences setup.

Furthermore time-invariant county-level unobservable factors drop out due to taking a difference in county-level outcomes. Unbiased estimates require that wind exposure measure is not correlated with time-varying unobservables that also affect outcomes of interest. We estimate the following long differences model:

$$\Delta y_i = \beta_{LD} w_i + \lambda \mathbf{X}_i + \psi_s + \Delta \epsilon_i \quad (4)$$

where Δy_i is the change in some outcome y in county i between two periods. We take averages of each outcome y over 1930-1935 and 1960-1965 and difference these averages to arrive at Δy_i . As before, w_i is the wind exposure measure that approximates exposure to summer winds from the afforested Shelterbelt counties. We also include state fixed effects,

ψ_s , to control for unobserved state-level trends, as well as the same county-level controls (\mathbf{X}_i) as in our main specification (Equation 1).

All of our long differences estimates are generally consistent with our difference-in-differences estimates: we find rainfall increased and temperatures decreased with higher exposure to winds from the Shelterbelt. Corn production and area harvested also increased. The results are robust regardless of including controls or not (Figure 4).

Binary treatment variables: In addition to our main specification where we use the exposure to summer winds from afforested areas as a continuous treatment variable, we also replicate our results using binary treatment measures. While this approach is not able to take advantage of all the variation in the wind exposure measure, it allows us to conduct helpful placebo exercises. We still use our wind exposure measure, but now classify counties into the following groups:

- i) Shelterbelt counties, with concentrated windbreak planting covering at least 5% of county area
- ii) Downwind neighbor counties, with centroids within 200km of Shelterbelt counties and above median wind exposure from afforested areas²⁰
- iii) Other neighbor counties, with centroids within 200km of Shelterbelt counties and below median wind exposure from afforested areas
- iv) Pure control counties, with centroids 200-300km away from Shelterbelt counties

We compare climate and economic outcomes across these four groups of counties. We define the local effects of tree planting as the impacts on the Shelterbelt counties themselves, while the regional effects are the impacts on the neighboring downwind counties. We expect little to no effect on the climate of the other (non-downwind) counties. We therefore use them as a placebo test when considering climate outcomes.

We first estimate the following difference-in-differences Equation:

$$y_{it} = \beta_{D1}(S_i \times P_t) + \beta_{D2}(D_i \times P_t) + \beta_{D3}(U_i \times P_t) + \gamma(\mathbf{X}_i \times Y_t) + \gamma_{st} + \nu_i + \epsilon_{it} \quad (5)$$

where S_i is an indicator for Shelterbelt counties, D_i is an indicator for downwind neighbor counties, and U_i is an indicator for other neighbor counties. As before, we add time-invariant county-level controls interacted by year, as well as state-by-year (γ_{st}) and county (ν_i) fixed effects.

²⁰ See Appendix Figure A12 for the distribution of wind exposure measures for neighbor counties.

In addition to the difference-in-differences specification, we also implement a version of the long differences approach previously described. Again, instead of using the continuous treatment variable (w_i), we use the binary treatment variables and estimate:

$$\Delta y_i = \beta_{LDD1} S_i + \beta_{LDD2} D_i + \beta_{LDD3} U_i + \lambda \mathbf{X}_i + \psi_s + \Delta \epsilon_i \quad (6)$$

In Equation 5(6), our coefficients of interest are $\beta_{D1}(\beta_{LDD1})$ and $\beta_{D2}(\beta_{LDD2})$, which measure the change in post-1942 outcomes relative to control counties for Shelterbelt and downwind counties, respectively. $\beta_{D1}(\beta_{LDD1})$ is the local effect of tree planting among Shelterbelt counties, while $\beta_{D2}(\beta_{LDD2})$ is the spillover effect of tree planting among downwind neighbors. The effect on other neighboring counties is $\beta_{D3}(\beta_{LDD3})$ and is expected to be zero, and serves as a placebo test.²¹

Figure 6 summarizes our results with the binary treatment variables. Overall, we find very similar effects as in our main analyses using a continuous treatment measure. Summer precipitation increased while summer temperature decreased relative to control counties both in Shelterbelt and downwind neighboring counties. Reassuringly, rainfall and temperature are not affected in other other, non-downwind neighboring counties. Large reductions occur in degree days above 29°C.

The results for economic outcomes are also consistent with our main results that use the continuous wind exposure treatment variable. We find that corn production and area harvested increases in Shelterbelt counties. Importantly, the same is true in downwind neighboring counties, without afforestation. As before, changes in downwind counties identify changes due to improved climate conditions alone. Notably, the difference between downwind and other neighbor effects is positive and statistically significant in most specifications, meaning that improved climate conditions alone—without other mechanisms such as direct soil benefits of tree planting or general equilibrium effects—lead to higher production, area harvested, and yields in areas downwind of afforestation.²²

²¹ The binary treatment setup also allows us to conduct a synthetic difference-in-differences analysis, addressing potential concerns with parallel trends. Appendix Section A.6 describes this approach and the results (shown in Appendix Tables A8 and A9).

²² A 1955 survey in South Dakota estimated direct local effects, reporting corn yields of 8 bushels per acre higher in fields next to shelterbelts compared to non-shelterbelt fields, or about 30% of average yields in South Dakota during that period (Ferber et al. 1955).

5.4 Internal validity

We now consider factors other than the Shelterbelt that could threaten the internal validity of our results, by potentially explaining the climate and economic effects we find.

Wind: Spatially consistent wind data are only available beginning 1979. As such, our classification of counties into “downwind neighbors” and “other neighbors” cannot be based on baseline data. Instead, we derive it from long-term prevailing wind patterns computed over 1981-2010. We test whether our results could partly be driven by this classification using ex-post data.

Direct empirical evidence suggests that prevailing winds have remained stable throughout our study period. Our classification of counties would thus have likely been similar, had baseline data been available. First, we construct an alternative measure of wind exposure, based on 1938-1942 data from the available weather stations in our study area that monitored wind.²³ We find a correlation of 0.92 between the two measures—indicating that wind exposure from the Shelterbelt has been stable throughout the period (Figure A10). Going one step further and implementing a long differences empirical strategy on this subsample of observations, we do not find evidence that Shelterbelt tree planting affects this wind measure.

Beyond this direct evidence, the pattern of our main results is inconsistent with a bias induced by a misclassification of counties from the use of post-intervention wind data. Assume indeed that the Shelterbelt tree planting changes wind patterns in a way that affects climate in neighboring counties. Then, a bias would occur if we classify as downwind neighbor areas that now receive precipitation from the new wind regime but didn’t before. However, this new precipitation would be reallocated towards the downwind neighbors from counties that we classify as other non-downwind neighbors: they used to receive precipitation from the wind, but do not anymore due to the new wind pattern. Then, if the Shelterbelt tree planting were affecting wind patterns in a way that reallocates precipitation, we should observe an effect of the intervention on the downwind neighbor counties of the same magnitude and opposite direction than the effect on the other non-downwind neighbor counties. But since we do not find a negative treatment effect on other non-downwind neighbor counties, it is unlikely that there was any material reallocation of precipitation.

Taken together, these results suggest that classifying neighboring counties based on wind data from the post-intervention period is unlikely to be biasing our estimates.

Irrigation: If irrigation is correlated with tree planting, it may be that our results are in fact

²³ The construction procedure is described in Appendix A.2. This exercise cannot be meaningfully conducted before 1938, due to the sparsity of weather station data in the Great Plains region then.

driven by changes in local climate from irrigation as opposed to afforestation. Like trees, irrigation can increase local evapotranspiration and thus influence the local climate (e.g., Lobell et al. 2008; DeAngelis et al. 2010; Mueller et al. 2016; Braun and Schlenker 2023). There are two concerns: first, that the trees planted as part of the Shelterbelt may have been directly irrigated, and second, that afforested and downwind neighboring lands were more likely to be irrigated, but not the Shelterbelt trees themselves. When discussing cultivation of Shelterbelt windbreaks, Barton (1936) describes the preparation of the ground to store precipitation as well as clean cultivation in years after planting (i.e., getting rid of grass and weeds under seedlings), but there is no mention of irrigation. The contemporaneous account shows windbreaks were very unlikely to be irrigated, as water was scarce and irrigation did not expand in earnest until the post-war period.

To address the second concern, we plot the concentrated shelterbelt planting and wind exposure measure against the share of area irrigated before and after planting at the county level (Figure A13). The areas that become irrigated are orthogonal to both the areas planted under the Shelterbelt program, and the areas downwind from the Shelterbelt. As a further test, we also replicate our long differences analyses (Equation 4) with the change in the share of land between 1935 and 1959 as a dependent variable. The results of this analysis are shown in Appendix Table A10. Even though irrigated areas and Shelterbelt planting are orthogonal at the county level, counties more exposed to winds from afforested areas see an increase in the share of irrigated land during this time period (Appendix Table A10, Column (1)). However, when we include the set of time-invariant controls from our main specification, the increase is no longer statistically significant (Appendix Table A10, Column (2)).

Regardless, we conduct more analysis to show that irrigation is not driving our main results. Almost all of the increase in irrigation in the region was attributed to the Ogallala aquifer. Therefore, we interact the wind exposure term in our main regression (Equation 1) with a dummy variable set to 1 for counties within the Ogallala. We find similar improvements in growing conditions both outside and inside the Ogallala aquifer (Appendix Table A11). We also find large increases in corn production and area (Appendix Table A12, Columns (1) and (2)) in both regions. However, the increase in corn yields is limited to the Ogallala region. As the corn area harvested increased in counties with an improved climate, farmers moved to marginal lands, and corn yields did not increase outside of Ogallala (Appendix Table A12, Column (3)). However, in the Ogallala, irrigation may have allowed farmers to take further advantage of improved climate conditions even on marginal lands, leading to increases in yields. As such, although irrigation has the potential to influence the local climate, it is

unlikely to confound our results.

Dust Bowl and medium-term climate fluctuations: Finally, we consider a potential threat to the identifying assumption of parallel trends: that the groups of counties considered were exposed to different weather shocks or medium-term climate patterns. The Shelterbelt project was indeed conceived and implemented in reaction to the Dust Bowl—a major climatic episode that spanned much of the 1930s.²⁴ One might wonder, consequently, whether a reversion to non-shock conditions might have occurred around the time of the tree planting. More broadly, it is well established that oceanic oscillations influence regional climate over the course of years and decades. The most prominent is the El Niño-Southern Oscillation (ENSO) in which warming in the Pacific Ocean produces periodic climate shifts that differentially affect regions across the globe (Zebiak and Cane 1987). These fluctuations might then differentially affect the counties in our sample.

Reassuringly, the counties affected and non-affected by winds from the Shelterbelt project exhibit parallel trends in the baseline period. Nonetheless, the counties affected appear to be drier and have more extreme temperatures than control counties, on average (Figure 3). Despite the observed parallel trends, there remains a concern that differential exposure to a decennial weather shock during the baseline period could induce this level difference across the affected and control counties. We address this concern in several ways.

First, we expand the time span of our analysis further back in time, and replicate our main analysis by comparing affected and control counties facing the same medium-term climate fluctuations. Our main analysis starts in 1930, a choice driven by concerns about the availability and quality of pre-1930 climate and agricultural data (Knappenberger et al. 2001; Kunkel et al. 2007). With that caveat, we use the available climate data from 1910 onward for this exercise.²⁵ There appear to be different pre-exposure trends between Shelterbelt and control counties in the 1910s and 1920s, leading up to the differential levels observed in the 1930s (Appendix Figure A16). We note that replicating our main difference-in-differences analysis for 1910 through 1965 produces similar results to our main analysis, though somewhat less precise and lower in magnitude (Appendix Table A13). But given these divergent early-period pre-trends, we further focus on counties experiencing similar climate patterns from 1910 to 1942 (our pre-exposure period)—and since they do not experience

²⁴ Interestingly, climate scientists argue that the Dust Bowl of the 1930s was caused by a combination of oceanic anomalies (which are exogenous to human activities in the US Midwest) and of local human-induced land degradation (Cook et al. 2009).

²⁵ In order to replicate our analysis for 1910 through 1965, we repeat the construction of a county-by-year precipitation and temperature panel based on daily weather stations, except using a balanced panel of stations reporting between 1910 and 1965 instead of 1930 and 1965.

differential patterns, concerns about medium-term climate reversion are alleviated.

To this end, we repeat the synthetic difference-in-differences (binary treatment variables) approach for this longer time period.²⁶ By construction, the synthetic difference-in-differences control region experiences the same climate trends throughout the pre-treatment period as the treated counties.²⁷ Appendix Table A14 contains the results of the synthetic difference-in-differences analysis for the periods from 1910 to 1965 and 1919 to 1965. Despite our concerns about data quality in the early period, our main precipitation results in downwind counties remain robust in this version of the analysis. Temperature results are lower in magnitude but directionally consistent with our headline results.

Next, we also repeat our long differences analyses for alternate time periods. First, in Panel A of Appendix Table A15, we compare 1925-1930 – instead of 1930-1935 – to 1960-1965, to address concerns that the early 1930s were still heavy drought periods. Our results are very similar to our main long differences results presented in Figure 4. We also compare 1930-1935 to 1950-1955, to compare pre- and post-treatment drought periods in the Great Plains. Panel B of Appendix Table A15 shows that the effects on temperature are even greater when comparing these two dry periods. This highlights the importance of the Shelterbelts in building resilience to droughts in the region.

Finally, we take a completely different approach in addressing concerns about medium-term climate reversions. We repeat our analysis at a hyperlocal level, using individual weather station data and the shapefile of the exact location and area of surviving Shelterbelt plantings (Snow 2019) to calculate afforested area in the vicinity of each station. Variations in tree planting intensity at this very local level are uncorrelated or only weakly correlated with measures of Dust Bowl intensity. The hyperlocal comparison essentially allows us to control for climate patterns at broader spatial and temporal scales. We find that stations with more nearby afforestation recorded higher precipitation and lower temperatures in the decades after the Shelterbelt project (Appendix Table A16). These results, though likely partially mitigated by spillover effects that we document, show that the change in climate due to tree planting holds at the local level—and not just at spatial scales that could reflect multi-decadal climate phenomena such as oceanic oscillations. Further discussion of the station-level results is provided in Appendix A.5.

²⁶ See Section A.6 for more details.

²⁷ More precisely, the weighted pre-exposure climate trend will be the same for the treated units and the synthetic control units. The synthetic difference-in-differences graphs show that most pre-treatment periods receive non-zero weights.

6 Conclusion and discussion

While tree planting is often positioned as an important tool in mitigating global climate change, the impacts of massive tree-planting programs on local and regional climate—and resulting economic effects—are less often examined and discussed. In this paper, we study the Great Plains Shelterbelt project, which planted over 220 million trees in the US Midwest between 1935 and 1942, representing what is likely the largest afforestation initiative in history up to that date.

We digitize historical maps of the Shelterbelt project to study the effects of tree planting on precipitation and temperature and economic outcomes like yields. We use a difference-in-differences approach that exploits wind patterns. We compare counties more exposed to large-scale prevailing winds from afforested areas in the Shelterbelt to those less exposed to these winds. We find that rainfall increased and temperature decreased with higher exposure to winds from afforested areas. Our results are robust to various alternate empirical methods, including instrumental variables, long differences, and difference-in-differences with binary treatment variables, and synthetic difference-in-differences approaches.

Are these climate effects realistic given the scale of the tree-planting effort? One way to test this is to compare the precipitation effect we find in Table 1 to the theoretical transpiration rate of trees. Our estimated precipitation coefficient is 0.78 cm per month for a unit increase in wind exposure. Summing this over the three summer months that we analyze from June to August (2.35 cm), multiplying it by the average wind exposure in the total region studied (0.15), and multiplying by the total region studied ($1,694,433\text{km}^2$), results in an increase of 1 cm of water per year spread across $597,796\text{km}^2$, which is equivalent to 4.8 million acre-feet of water (1.58 trillion gallons). In terms of theoretical transpiration, the Shelterbelt program planted 220 million trees with an estimated survival rate of 61% (Read 1958). USGS estimates that a large oak tree can transpire 40,000 gallons per year.²⁸ Proportionally allocating across the three summer months equates to 10,000 gallons per tree per year. Thus the surviving 134 million trees could produce 1.34 trillion gallons of water via transpiration—which is remarkably consistent with the 1.58 trillion gallons attributable to increased precipitation. While this exercise is coarse and simplistic²⁹—the general alignment between the program’s estimated and physical potential is reassuring.

After establishing the climate effects of the Shelterbelt project, we turn to study the economic

²⁸ <https://www.usgs.gov/special-topics/water-science-school/science/evapotranspiration-and-water-cycle>

²⁹ This back-of-the-envelope calculation omits many important factors, including direct evaporation from the soil, interactions with cropland, and differential transpiration rates across tree species, baseline climate, and temporally across the growing season.

impacts of this engineered climate change. Our strategy enables us to disentangle the effect of a changing climate on economic outcomes from other mechanisms. We find that corn production, area planted, and yields increased in areas more exposed to winds from the Shelterbelt, but not directly afforested. We also observe adaptation to more favorable climate conditions as farmers reallocated pastureland. Furthermore, farmers switch from less water-sensitive crops like wheat to more water-sensitive crops like corn.

Our findings are especially timely given the global enthusiasm for large-scale tree planting as a means of mitigating climate change in light of estimates that such activities could potentially reduce atmospheric CO₂ levels by 25% (Bastin et al. 2019). Tree planting is a major part of nearly all proposed pathways to ‘net zero’ emissions, with estimated capital requirements on the scale of hundreds of billions of dollars. The excitement around tree planting is further evidenced by the increasing number of national forestry initiatives used by countries to meet their mitigation targets under the Paris Agreement.³⁰

There are good reasons for this enthusiasm. Tree planting is a ‘simple technology’ enjoying high levels of public approval. And prior to concerns about climate change, afforestation initiatives like the Great Plains Shelterbelt and China’s Three-North Shelterbelt Program were implemented to stabilize soils and reduce erosion and dust storms. Our paper adds another co-benefit to this list. The increased precipitation and decreased extreme heat that we find during the growing season provides a major benefit to most types of agricultural production—particularly in the major cropland regions of the world that face hot summers and limited rainfall—conditions that are worsening under climate change. So in this sense, tree planting can be both a tool for mitigation (by sequestering carbon), as well as adaptation (by reducing the negative impact of global warming on agriculture).³¹

However, large-scale afforestation is not without controversy, particularly regarding the enormous amount of land required to reduce CO₂ levels at a meaningful scale.³² Some critics

³⁰ Recently national initiatives include Pakistan’s 10 Billion Trees Tsunami (2018), India’s Tree-planting pledges (2017), Mexico’s Sowing Life Program (2019), Kazakhstan’s Two Billion Tree Project (2020), Turkey’s Breath for the Future (2021), Mongolia’s One Billion Tree Project (2021), and WEF’s One Trillion Trees (2020).

³¹ An active literature in economics focuses on the drivers and consequences of deforestation, especially in the tropics (Burgess et al. 2012; Jayachandran et al. 2017; Burgess et al. 2019; Balboni et al. 2021; Araujo et al. 2022). A forthcoming review is provided by Balboni et al., n.d. Our study focuses on tree planting, but the benefits we identify can also represent costs from deforestation. By illustrating the challenges to maintain the current tree cover, this evidence base can help guide the design of afforestation programs.

³² One estimate of the land required for afforestation to achieve a ‘net zero’ transition is 160 million hectares by 2030, larger than France, Spain, and Germany combined (McKinsey Global Institute 2022); another report estimated an even larger figure of 1.2 *billion* hectares to achieve the carbon sequestration from national climate pledges under the Paris Agreement—an area equivalent to all current global cropland (Dooley et al. 2022).

worry that massive afforestation efforts could come at the expense of cropland and thus food security, while others are concerned that about the dispossession of land from pastoralists and other traditional groups. Another major concern relates to the timing of the CO₂ reductions, given that emission reductions are immediate while trees take decades to grow, as well as their permanence in light of the potential for large-scale tree mortality from drought, invasive species (e.g., mountain pine beetle), cyclones, and wildfires (Leverkus et al. 2022).

Many of these very real concerns can be addressed through the careful design of afforestation programs. It is important to note that not all tree-planting initiatives are equal and that their outcomes and co-benefits will be a function of the land selected, the tree species included, their ongoing management over time, and community engagement. In China, there is evidence of farmers cutting down native trees and replacing them with monocultural plantations (Hua et al. 2018). The program we study, the Great Plains Shelterbelt, was unique in that tree planting occurred in concentrated areas and windbreaks. Over 30 species of trees and shrubs were selected—tall and short trees, fast and slow growing trees, hardwoods and conifers—most of which were native and thus locally adapted (Read 1958) to ensure species diversity and ecological resilience in a way that mimicked naturally-occurring forests. Clearly, a tree planting program involving monocultures or non-native species could produce outcomes different than what we find—as well as different capital costs.

Relatedly, another valid question concerns the external validity of our results and the extent that the Great Plains is similar to other potential tree planting regions of the world. In terms of economic status, we first note that many countries today are still highly dependent on agriculture like the US Midwest was in the 1940s.³³ In terms of agronomic conditions, the Great Plains Shelterbelt occurred on mollisol soils, which are common throughout rainfall-limited regions that were historically grasslands. As shown in Appendix Figure A15, these soils are also present in the major crop growing regions of China, Russia, Kazakhstan, Ukraine, Turkey, Argentina, Uruguay, Mexico, and Canada—many of the same countries which have proposed large-scale tree planting programs. Thus it is reasonable to think that similar climate and yield effects from tree planting could occur outside the Great Plains context.

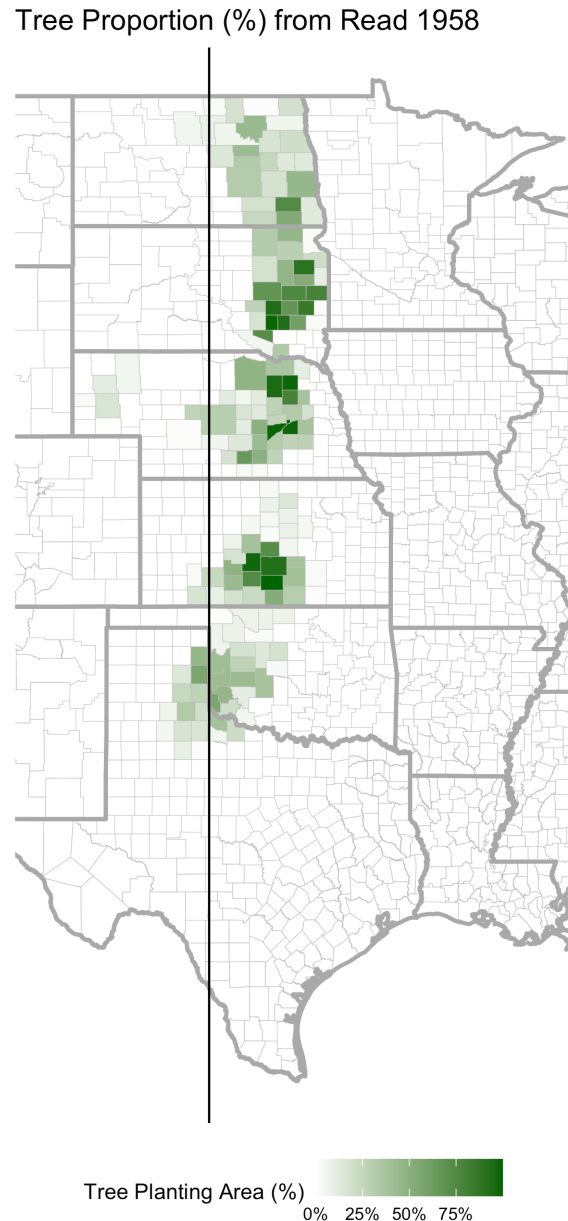
To conclude, we find that the Great Plains Shelterbelt altered the climate and growing conditions of a meaningfully large area—a region twice the size of California—over the course of several decades, producing important economic consequences. Our results show that human actions can alter local and regional climates through land use. In addition to the implications for tree planting initiatives and climate policy described above, our paper

³³ Both Mexico and China, for example, have a current GDP per capita and share of the population employed in agriculture similar to the US in 1940 (Appendix Figure A14).

highlights the endogeneity risk in using spatial variation in climate trends to assess local climate change impacts and the potential bias it can imbue on climate change damage estimates. Future work should investigate how drivers of climate spillovers can be used as instruments for identifying the effect of climate change on economic outcomes.

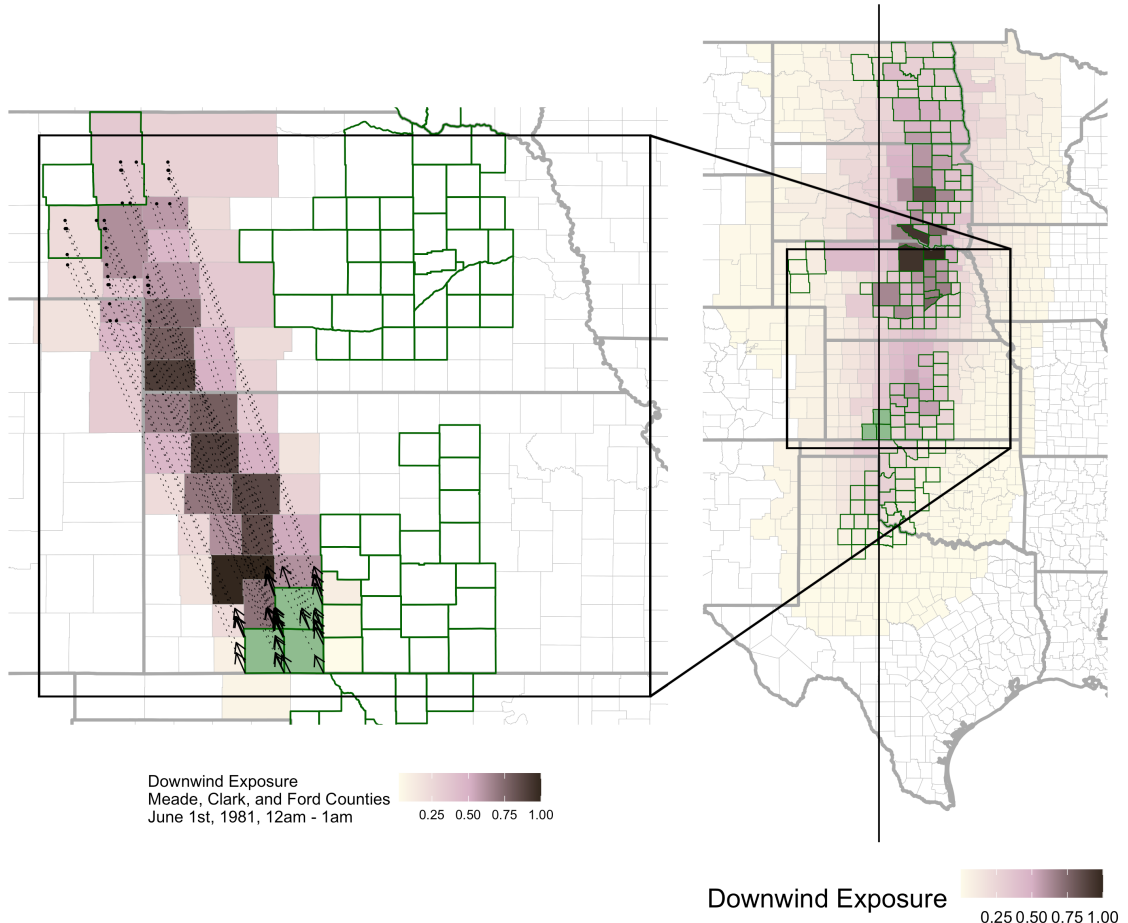
7 Figures

Figure 1: Shelterbelt measure



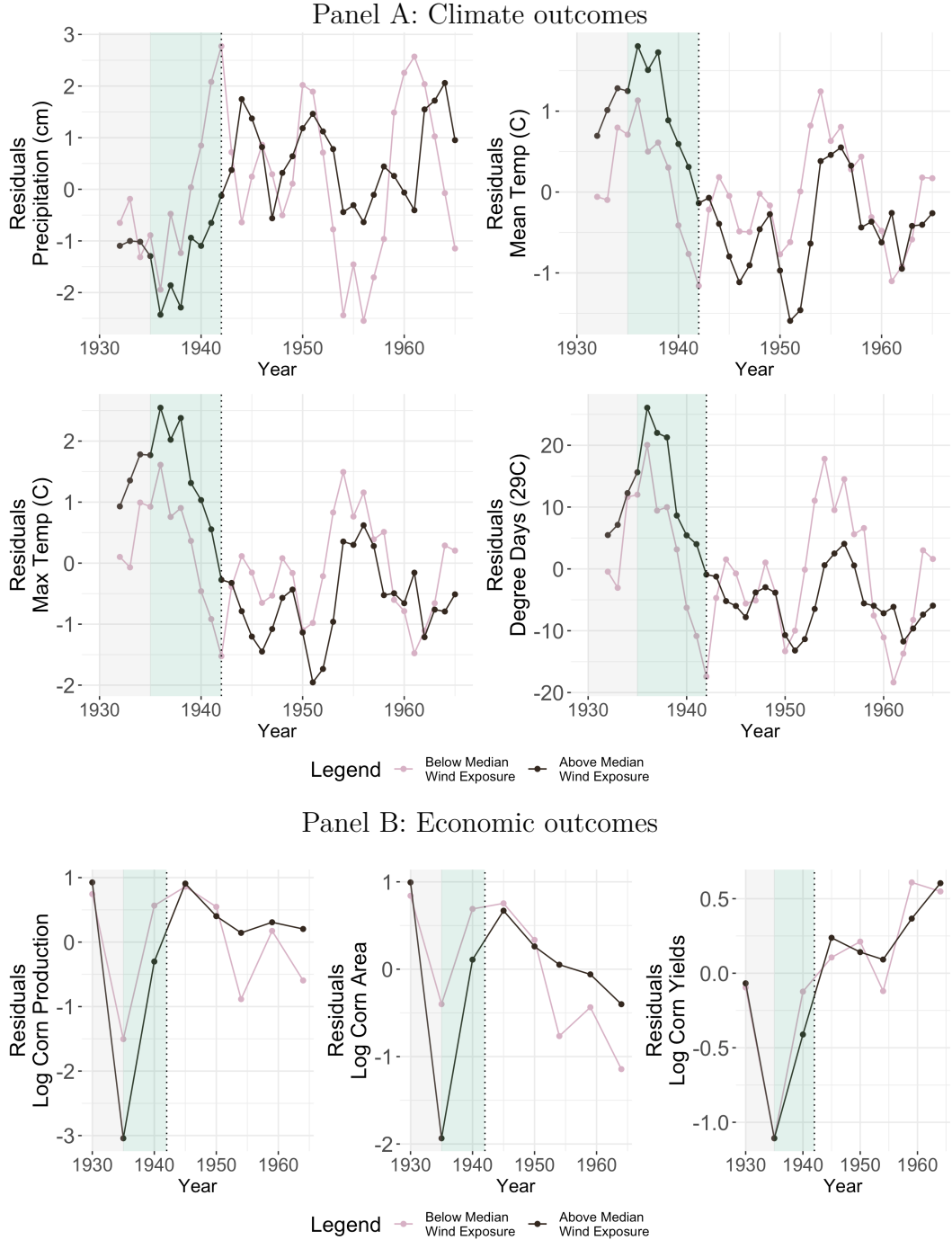
Notes: Figure shows intensive tree planting area (% of county area) based on digitized maps from Read (1958). We calculate the percentage of each county covered by “areas of concentrated Shelterbelt planting”. Throughout the paper, we refer to counties with at least 5% tree proportion as Shelterbelt counties.

Figure 2: Shelterbelt wind exposure measure



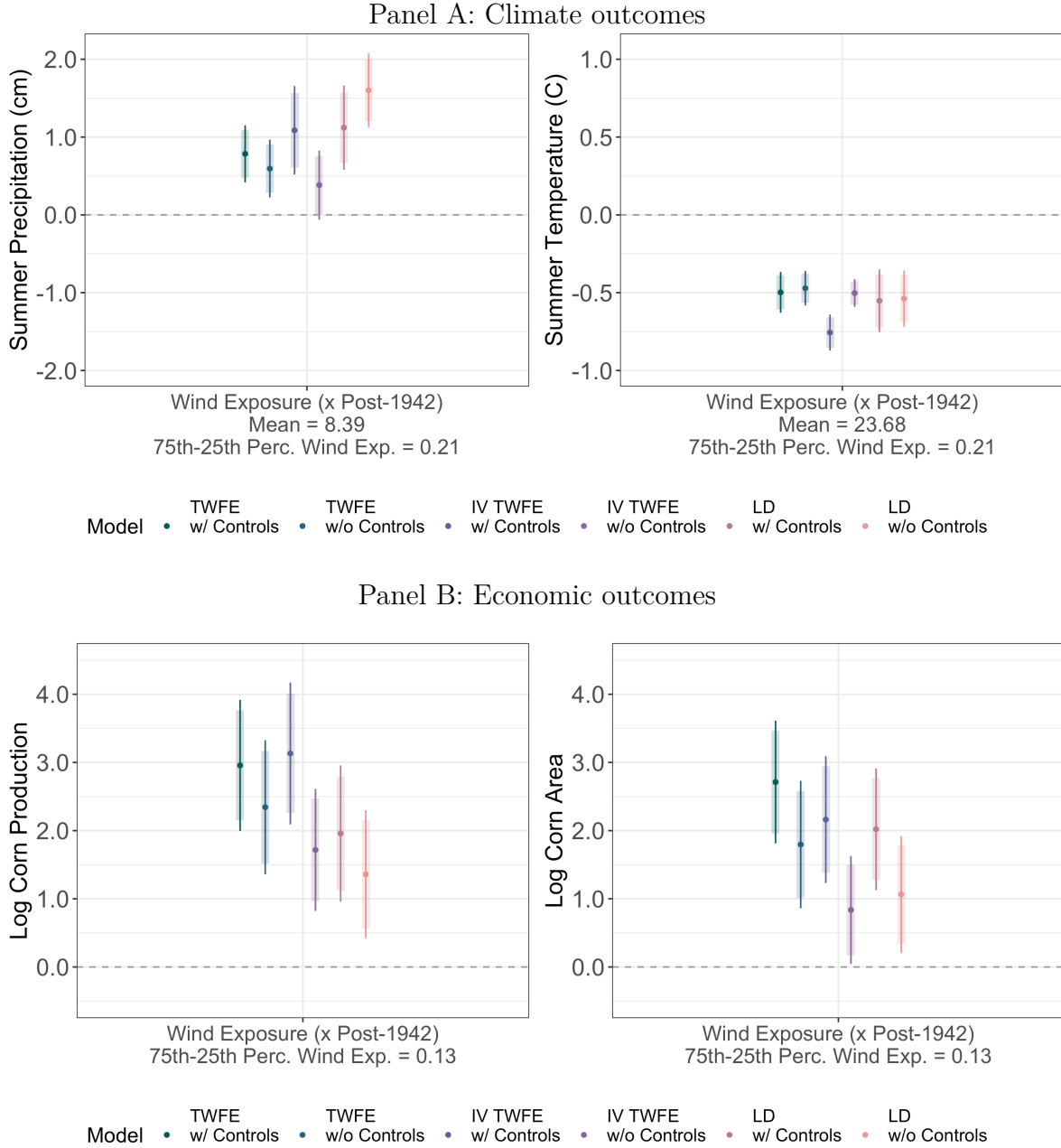
Notes: Figures illustrate the construction of our Shelterbelt wind exposure measure. Counties with green border are Shelterbelt counties while purple shading shows continuous wind exposure measure. Left panel shows detail in Kansas for three Shelterbelt counties (Meade, Clark, and Ford) for one hour. Arrows represent direction and magnitude of prevailing winds for a given hour, while dotted lines show the path of imaginary particles projected from county vertices. Neighboring counties that intersect more paths are counties with higher exposure to winds that pass through Shelterbelt areas. Our final wind exposure measure is a weighted sum of wind exposure for all summer hours and from all Shelterbelt counties. Exposure is also weighted based on the share of county covered by concentrated Shelterbelt planting. Right panel shows the final continuous wind exposure measure for all counties.

Figure 3: Trends in outcomes for low and high wind exposure counties



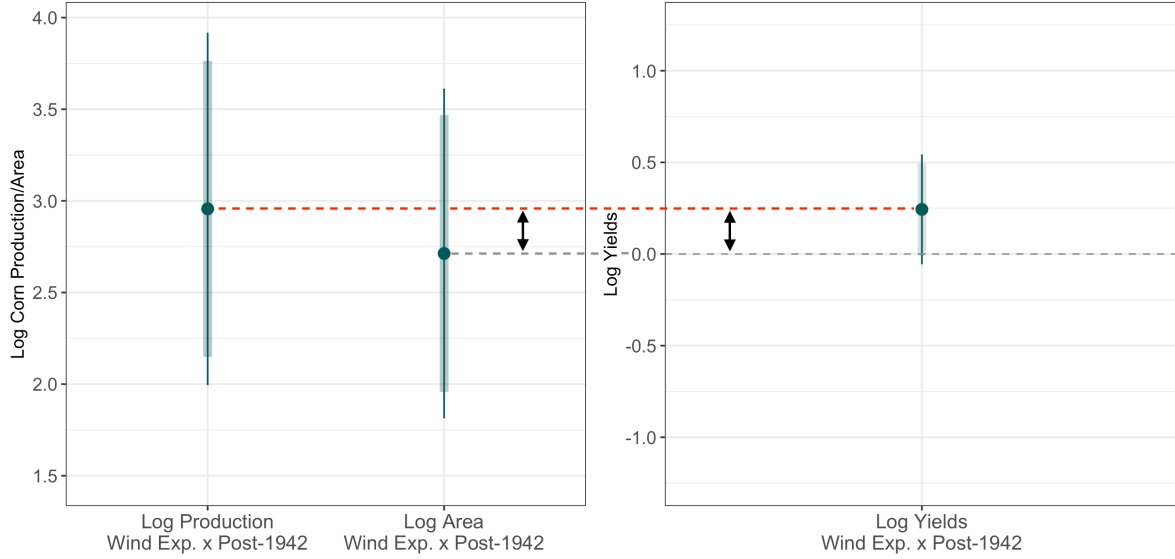
Notes: Figures plot average residuals for 1930-1965, for counties above and below the median wind exposure measure. Residuals shown after controlling for state and county fixed effects. Gray shaded area shows pure baseline period (without tree planting), green shaded area shows Shelterbelt project years. Panel A shows climate outcomes of summer precipitation, mean/maximum summer temperatures, and 29C degree days, with 3-year rolling averages used due to high variation in annual weather outcomes. Panel B shows (log) corn production, area harvested, and yields from USDA 5-year agricultural census.

Figure 4: Climate and economic results summary



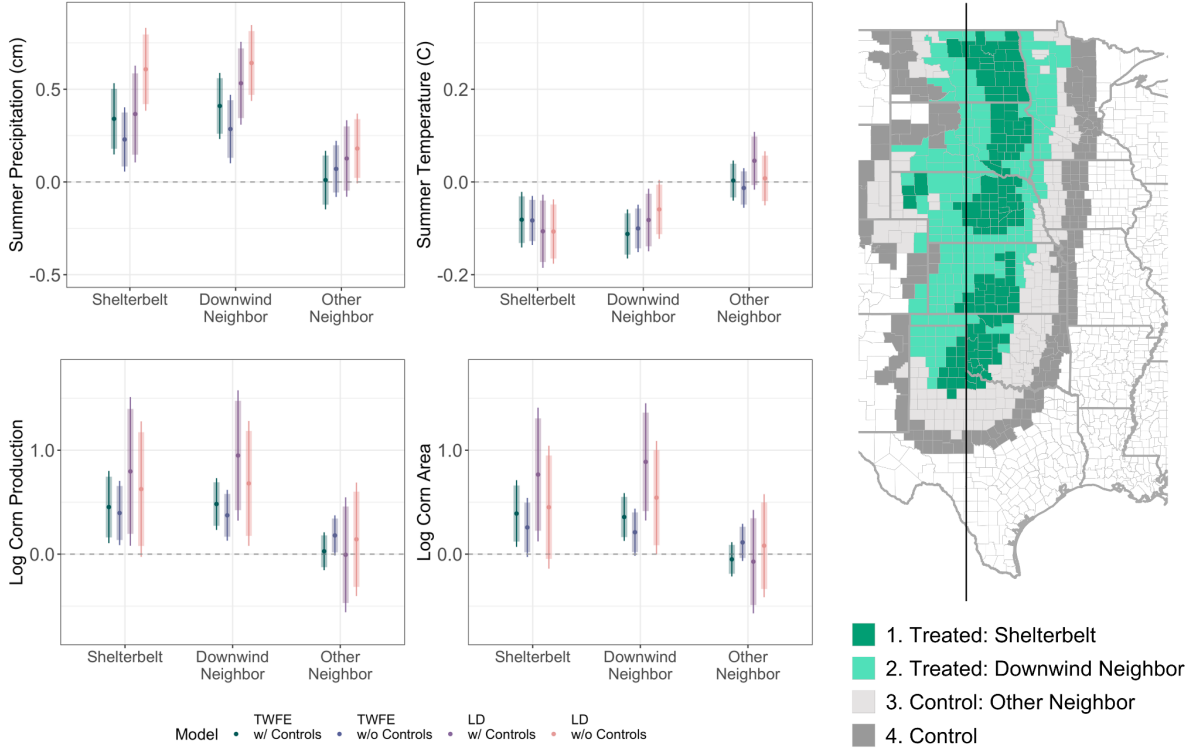
Notes: Figures plot coefficient estimates and 95% (thin line) and 90% (thick line) confidence intervals across three different models: TWFE (Equation 1), instrumental variables TWFE (Equation 3), long differences (LD) (Equation 4) each with and without controls. Main independent variable is wind exposure (w_i), which measures approximate exposure to winds from afforested areas, interacted by a post-treatment dummy for the TWFE models. “75th-25th Perc Wind Exp” shows the difference between the 75th and 25th percentile of the continuous wind exposure measure. Time-invariant controls include county-level crop suitability, soil characteristics, Dust Bowl erosion measures, and 1935 irrigation intensity. County and state-by-year (or state, for LD) FE included. In Panel A, dependent variables are summer precipitation and mean temperature (June - August averages). In Panel B, dependent variables are log corn production and area (left panel) using census data and log corn yields (right panel).

Figure 5: Corn production, area, and yield increase



Notes: Figures plot coefficient estimates and 95% (thin line) and 90% (thick line) confidence intervals for log corn production and area (left panel) using census data and log corn yields (right panel) for 481 counties, with centroids within 300km of the centroids of Shelterbelt counties, dropping directly afforested areas. Main independent variable is wind exposure (w_i), which measures approximate exposure to winds from afforested areas, interacted by a post-treatment dummy. Time-invariant controls, interacted by year, include county-level crop suitability, soil characteristics, Dust Bowl erosion measures, and 1935 irrigation intensity. County and state-by-year FE included. Figure demonstrates that the difference between log production increase and log area increase is equal to the log yield increase.

Figure 6: Results using binary treatment variables instead of continuous wind exposure measure



8 Tables

Table 1: Impact of Great Plains Shelterbelt on Jun-Aug county climate, 1930 to 1965

	<i>Dependent variable:</i>			
	Precipitation (cm)	Mean Temp (C)	Max Temp (C)	Degree Days (29C)
	(1)	(2)	(3)	(4)
Wind Exposure:Post 1942	0.784*** (0.187) [0.000]	-0.498*** (0.067) [0.000]	-0.842*** (0.098) [0.000]	-9.147*** (0.993) [0.000]
Mean	8.39	23.68	30.87	28.80
Std.Dev.	3.49	3.04	3.17	22.46
75th-25th Perc. Wind Exp	0.21	0.21	0.21	0.21
Observations	21,528	21,528	21,528	21,528

Notes: Standard errors clustered at the county level shown in parentheses; p-values shown in brackets (*p<0.1; **p<0.05; ***p<0.01). Table shows results for estimating Equation 1 for 678 counties, with centroids within 300km of the centroids of Shelterbelt counties. Dependent variables are June - August averages. Main independent variable is wind exposure (w_i), which measures approximate exposure to winds from afforested areas, interacted by a post-treatment dummy. “75th-25th Perc Wind Exp” shows the difference between the 75th and 25th percentile of the continuous wind exposure measure. Time-invariant controls, interacted by year, include county-level crop suitability, soil characteristics, Dust Bowl erosion measures, and 1935 irrigation intensity. County and state-by-year FE included.

Table 2: Impact of Great Plains Shelterbelt on corn production, area harvested, and yields using USDA 5-year agricultural census data, 1930 to 1964

	<i>Dependent variable:</i>		
	Log Production	Log Area	Log Yields
	(1)	(2)	(3)
Wind Exposure:Post 1942	2.956*** (0.489) [0.000]	2.713*** (0.458) [0.000]	0.243 (0.152) [0.111]
75th-25th Perc. Wind Exp	0.13	0.13	0.13
Observations	3,597	3,597	3,597

Notes: Standard errors clustered at the county level shown in parentheses; p-values shown in brackets (*p<0.1; **p<0.05; ***p<0.01). Table shows results for estimating Equation 1 for 481 counties, with centroids within 300km of the centroids of Shelterbelt counties, dropping directly afforested areas. Dependent variables are from USDA 5-year agricultural censuses (8 censuses between 1930 and 1964). Main independent variable is wind exposure (w_i), which measures approximate exposure to winds from afforested areas, interacted by a post-treatment dummy. “75th-25th Perc Wind Exp” shows the difference between the 75th and 25th percentile of the continuous wind exposure measure. Time-invariant controls, interacted by year, include county-level crop suitability, soil characteristics, Dust Bowl erosion measures, and 1935 irrigation intensity. County and state-by-year FE included.

Table 3: Impact of Great Plains Shelterbelt on agricultural land use, using USDA 5-year agricultural census data, 1930 to 1964

	<i>Dependent variable:</i>				
	Cropland	Pastureland (1000 ac)	Farmland	Corn Share	Wheat Share (% of Cropland)
	(1)	(2)	(3)	(4)	(5)
Wind Exposure:Post 1942	23.364 (22.986) [0.310]	-113.407 (143.571) [0.430]	-86.539** (39.806) [0.031]	0.108*** (0.021) [0.000]	-0.045* (0.026) [0.090]
75th-25th Perc. Wind Exp	0.13	0.13	0.13	0.13	0.13
Observations	3,728	3,728	3,728	3,723	3,562

Notes: Standard errors clustered at the county level shown in parentheses; p-values shown in brackets (*p<0.1; **p<0.05; ***p<0.01). Table shows results for estimating Equation 1 for 481 counties, with centroids within 300km of the centroids of Shelterbelt counties, dropping directly afforested areas. Dependent variables are from USDA 5-year agricultural censuses (8 censuses between 1930 and 1964). Main independent variable is wind exposure (w_i), which measures approximate exposure to winds from afforested areas, interacted by a post-treatment dummy. “75th-25th Perc Wind Exp” shows the difference between the 75th and 25th percentile of the continuous wind exposure measure. Time-invariant controls, interacted by year, include county-level crop suitability, soil characteristics, Dust Bowl erosion measures, and 1935 irrigation intensity. County and state-by-year FE included.

Table 4: Changes in climate and implied changes in corn yields

	<i>Dependent variable:</i>				
	Degree Days			Precipitation	Log Yields
	10C (1)	29C (2)	39C (3)	(cm) (4)	Implied (5)
Wind Exposure:Post 1942	-26.730*** (2.913) [0.000]	-14.532*** (1.330) [0.000]	-1.715*** (0.175) [0.000]	1.666*** (0.290) [0.000]	0.289 - -
75th-25th Perc. Wind Exp	0.13	0.13	0.13	0.13	0.13
Observations	16,776	16,776	16,776	16,776	-

Notes: Standard errors clustered at the county level shown in parentheses; p-values shown in brackets (*p<0.1; **p<0.05; ***p<0.01). Columns (1) - (4) of the table show results for estimating Equation 1 for 481 counties, with centroids within 300km of the centroids of Shelterbelt counties, dropping directly afforested areas. Main independent variables are variables used to estimate the weather-yield relationship (Equation 7, Appendix Table A5) based on Schlenker and Roberts (2009). Regressions include county and state-by-year FE. Column (5) shows the implied change in yields calculated using the steps described in Appendix A.4.

References

- Alkama, Ramdane, and Alessandro Cescatti. 2016. “Biophysical climate impacts of recent changes in global forest cover.” *Science* 351 (6273): 600–604.
- Annan, Francis, and Wolfram Schlenker. 2015. “Federal crop insurance and the disincentive to adapt to extreme heat.” *The American Economic Review Papers and Proceedings* 105 (5): 262–66.
- Araujo, Rafael. 2023. “When clouds go dry: an integrated model of deforestation, rainfall, and agriculture.”
- Araujo, Rafael, Francisco Costa, and Marcelo Sant’Anna. 2022. “Efficient forestation in the Brazilian Amazon: Evidence from a dynamic model.”
- Arkhangelsky, Dmitry, Susan Athey, David A. Hirshberg, Guido W. Imbens, and Stefan Wager. 2021. “Synthetic Difference-in-Differences.” *The American Economic Review* 111 (12): 4088–4118.
- Asher, Sam, Alison Campion, Douglas Gollin, and Paul Novosad. 2022. “The long-run development impacts of agricultural productivity gains: Evidence from irrigation canals in india.” *Working Paper*.
- Auffhammer, Maximilian. 2022. “Climate Adaptive Response Estimation: Short and long run impacts of climate change on residential electricity and natural gas consumption.” *Journal of Environmental Economics and Management* 114:102669.
- Balboni, Clare, Aaron Berman, Robin Burgess, Benjamin A Olken, Brian Copeland, Robert Heilmayr, Allan Hsiao, et al. n.d. “The economics of tropical deforestation.” Prepared, *Annual review of economics*.
- Balboni, Clare, Robin Burgess, and Benjamin A Olken. 2021. “The origins and control of forest fires in the tropics.”
- Barton, Thomas F. 1936. “The Great Plains Tree Shelterbelt Project.” *Journal of Geography* 35:125.
- Bastin, Jean-Francois, Yelena Finegold, Claude Garcia, Danilo Mollicone, Marcelo Rezende, Devin Routh, Constantin M Zohner, and Thomas W Crowther. 2019. “The global tree restoration potential.” *Science* 365 (6448): 76–79.
- Blakeslee, David, Ram Fishman, and Veena Srinivasan. 2020. “Way Down in the Hole: Adaptation to Long-Term Water Loss in Rural India.” *The American Economic Review* 110 (1): 200–224.
- Bonan, Gordon B. 2008. “Forests and Climate Change: Forcings, Feedbacks, and the Climate Benefits of Forests.” *Science* 320 (5882): 1444–1449.
- Braun, Thomas, and Wolfram Schlenker. 2023. “Cooling Externality of Large-Scale Irrigation.” *NBER Working Paper*, Working Paper Series, no. 30966.
- Burgess, Robin, Francisco J M Costa, and Ben Olken. 2019. “The Brazilian Amazon’s double reversal of fortune.”
- Burgess, Robin, Matthew Hansen, Benjamin A Olken, Peter Potapov, and Stefanie Sieber. 2012. “The Political Economy of Deforestation in the Tropics.” *The quarterly journal of economics* 127 (4): 1707–1754.
- Burke, Marshall, and Kyle Emerick. 2016. “Adaptation to climate change: Evidence from US agriculture.” *American Economic Journal: Economic Policy* 8 (3): 106–40.
- Burlig, Fiona, Louis Preonas, and Matt Woerman. 2021. “Energy, Groundwater, and Crop Choice.” *NBER Working Paper*, no. 28706.
- Bustos, Paula, Bruno Caprettini, and Jacopo Ponticelli. 2016. “Agricultural productivity and structural transformation: Evidence from Brazil.” *The American Economic Review*.
- Bustos, Paula, Gabriel Garber, and Jacopo Ponticelli. 2020. “Capital accumulation and structural transformation.” *The Quarterly Journal of Economics*.

- Butler, Ethan E, and Peter Huybers. 2013. "Adaptation of US maize to temperature variations." *Nature Climate Change* 3 (1): 68–72.
- Callaway, Brantly, Andrew Goodman-Bacon, and Pedro H. C. Sant'Anna. 2021. *Difference-in-Differences with a Continuous Treatment*. arXiv: 2107.02637 [econ.EM].
- Carleton, Tamara A., and Solomon M. Hsiang. 2016. "Social and economic impacts of climate." *Science* 353 (6304): aad9837.
- Cook, Benjamin I., Ron L. Miller, and Richard Seager. 2009. "Amplification of the North American Dust Bowl drought through human-induced land degradation." *Proceedings of the National Academy of Sciences* 106 (13): 4997–5001.
- Costinot, Arnaud, Dave Donaldson, and Cory Smith. 2016. "Evolving Comparative Advantage and the Impact of Climate Change in Agricultural Markets: Evidence from 1.7 Million Fields around the World." *Journal of Political Economy* 124 (1): 205–248. <https://doi.org/10.1086/684719>.
- Cui, Xiaomeng. 2020. "Climate change and adaptation in agriculture: Evidence from US cropping patterns." *Journal of Environmental Economics and Management* 101:102306.
- DeAngelis, Anthony, Francina Dominguez, Ying Fan, Alan Robock, M Deniz Kustu, and David Robinson. 2010. "Evidence of enhanced precipitation due to irrigation over the Great Plains of the United States." *Journal of Geophysical Research: Atmospheres* 115 (D15).
- Dell, Melissa, Benjamin F Jones, and Benjamin A Olken. 2012. "Temperature Shocks and Economic Growth: Evidence from the Last Half Century." *American Economic Journal: Macroeconomics* 4 (3): 66–95.
- . 2014. "What Do We Learn from the Weather? The New Climate-Economy Literature." *Journal of Economic Literature* 53 (3): 740–798.
- Deryugina, Tatyana, Garth Heutel, Nolan H. Miller, David Molitor, and Julian Reif. 2019. "The Mortality and Medical Costs of Air Pollution: Evidence from Changes in Wind Direction." *The American Economic Review* 109 (12): 4178–4219.
- Devaraju, N., Govindasamy Bala, and Angshuman Modak. 2015. "Effects of large-scale deforestation on precipitation in the monsoon regions: remote versus local effects." *Proceedings of the National Academy of Sciences* 112 (11): 3257–3262.
- Dooley, Kate, Heather Keith, Anne Larson, Georgina Catacora-Vargas, Wim Carton, Kirstine Lund Christiansen, Ojong Enokenwa Baa, Alain Frechette, Sonia Hugh, Nathan Ivetic, et al. 2022. "The Land Gap Report."
- Droze, Wilmon H. 1977. *Trees, prairies, and people: A history of tree planting in the Plains States*. Texas Woman's University.
- Ferber, Arthur E, AL Ford, and SA McCrory. 1955. "Good windbreaks help increase South Dakota crop yields."
- Georgescu, Matei, David B Lobell, and Christopher B Field. 2011. "Direct climate effects of perennial bioenergy crops in the United States." *Proceedings of the National Academy of Sciences* 108 (11): 4307–4312.
- Haines, Michael, Price Fishback, and Paul Rhode. 2018. *United States Agriculture Data, 1840 - 2012*.
- Heutel, Garth, Nolan H Miller, and David Molitor. 2021. "Adaptation and the mortality effects of temperature across US climate regions." *Review of Economics and Statistics* 103 (4): 740–753.
- Hornbeck, Richard. 2012. "The enduring impact of the American Dust Bowl: Short-and long-run adjustments to environmental catastrophe." *The American Economic Review* 102 (4): 1477–1507.

- Hornbeck, Richard, and Pinar Keskin. 2014. "The historically evolving impact of the Ogallala aquifer: Agricultural adaptation to groundwater and drought." *American Economic Journal: Applied Economics* 6 (1): 190–219.
- Hornbeck, Richard, and Enrico Moretti. 2023. "Estimating who benefits from productivity growth: local and distant effects of city productivity growth on wages, rents, and inequality." Forthcoming, *The Review of Economics and Statistics*.
- Horner, GM, WA Starr, and JK Patterson. 1957. "The Pacific Northwest wheat region." *The Yearbook of Agriculture (Washington, DC: US Department of Agriculture)*, 475–481.
- Howlader, Aparna. 2023. "Determinants and consequences of large-scale tree plantation projects: Evidence from the Great Plains Shelterbelt Project." *Land Use Policy* 132:106785.
- Hsiang, Solomon. 2016. "Climate Econometrics." *Annual Review of Resource Economics* 8 (1): 43–75.
- Hua, Fangyuan, Lin Wang, Brendan Fisher, Xinlei Zheng, Xiaoyang Wang, W Yu Douglas, Ya Tang, Jianguo Zhu, and David S Wilcove. 2018. "Tree plantations displacing native forests: The nature and drivers of apparent forest recovery on former croplands in Southwestern China from 2000 to 2015." *Biological Conservation* 222:113–124.
- Hultgren, Andrew, Tamara Carleton, Michael Delgado, Diana R Gergel, Michael Greenstone, Trevor Houser, Solomon Hsiang, Amir Jina, Robert E Kopp, Steven B Malevich, et al. 2022. "Estimating global impacts to agriculture from climate change accounting for adaptation." Available at SSRN 4222020.
- IPCC. 2019. "IPCC Special Report on the Ocean and Cryosphere in a Changing Climate [H.-O. Pörtner, D.C. Roberts, V. Masson-Delmotte, P. Zhai, M. Tignor, E. Poloczanska, K. Mintenbeck, A. Alegría, M. Nicolai, A. Okem, J. Petzold, B. Rama, N.M. Weyer]."
- Jayachandran, Seema, Joost de Laat, Eric F Lambin, Charlotte Y Stanton, Robin Audy, and Nancy E Thomas. 2017. *Cash for carbon: A randomized trial of payments for ecosystem services to reduce deforestation*, 6348.
- Kala, Namrata. 2017. "Learning, adaptation, and climate uncertainty: Evidence from Indian agriculture." *MIT Center for Energy and Environmental Policy Research Working Paper* 23.
- Kline, Patrick, and Enrico Moretti. 2014. "Local economic development, agglomeration economies, and the big push: 100 years of evidence from the Tennessee Valley Authority." *Quarterly Journal of Economics*.
- Knappenberger, Paul C., Patrick J. Michaels, and Robert E. Davis. 2001. "Nature of observed temperature changes across the United States during the 20th century." *Climate Research* 17 (1): 45–53.
- Koch, Alexander, Chris Brierley, Mark M Maslin, and Simon L Lewis. 2019. "Earth system impacts of the European arrival and Great Dying in the Americas after 1492." *Quaternary Science Reviews* 207:13–36.
- Kolstad, Charles D, and Frances C Moore. 2020. "Estimating the Economic Impacts of Climate Change Using Weather Observations." *Review of Environmental Economics and Policy* 14 (1): 1–24.
- Kunkel, Kenneth E., Michael A. Palecki, Kenneth G. Hubbard, David A. Robinson, Kelly T. Redmond, and David R. Easterling. 2007. "Trend Identification in Twentieth-Century U.S. Snowfall: The Challenges." *Journal of Atmospheric and Oceanic Technology* (Boston MA, USA) 24 (1): 64–73.
- Kurukulasuriya, Pradeep, and Robert Mendelsohn. 2008. "Crop switching as a strategy for adapting to climate change." *African Journal of Agricultural and Resource Economics* 2 (311-2016-5522): 105–126.
- Lemoine, Derek. 2021. "Estimating the Consequences of Climate Change from Variation in Weather." *NBER Working Paper*, Working Paper Series, no. 25008.
- Leverkus, Alejandro B, Simon Thorn, David B Lindenmayer, and Juli G Pausas. 2022. "Tree planting goals must account for wildfires." *Science* 376 (6593): 588–589.

- Li, Tianshu. 2021. "Protecting the breadbasket with trees? The effect of the great plains shelterbelt project on agriculture." *Land Economics* 97 (2): 321–344.
- Liu, Maggie, Yogita Shamdasani, and Vis Taraz. Forthcoming. "Climate Change and Labor Reallocation: Evidence from Six Decades of the Indian Census." *American Economic Journal: Economic Policy*.
- Loarie, S R, D B Lobell, G P Asner, Q Mu, et al. 2011. "Direct impacts on local climate of sugar-cane expansion in Brazil." *Nature climate change*.
- Lobell, David B, Celine J Bonfils, Lara M Kueppers, and Mark A Snyder. 2008. "Irrigation cooling effect on temperature and heat index extremes." *Geophysical Research Letters* 35 (9).
- Malikov, Emir, Ruiqing Miao, and Jingfang Zhang. 2020. "Distributional and temporal heterogeneity in the climate change effects on U.S. agriculture." *Journal of environmental economics and management* 104:102386.
- McKinsey Global Institute. 2022. *The net-zero transition: what it would cost, what it could bring*. Technical report. <https://www.mckinsey.com/capabilities/sustainability/our-insights/the-net-zero-transition-what-it-would-cost-what-it-could-bring>.
- Montesquieu, Charles de. 1750. *The Spirit of the Laws*. Thomas Nugent.
- Mueller, Nathaniel D, Ethan E Butler, Karen A McKinnon, Andrew Rhines, Martin Tingley, N Michele Holbrook, and Peter Huybers. 2016. "Cooling of US Midwest summer temperature extremes from cropland intensification." *Nature Climate Change* 6 (3): 317–322.
- Munns, E. N., and Joseph H. Stoeckeler. 1946. "How Are the Great Plains Shelterbelts?" *Journal of Forestry* 44 (4): 237–257.
- Neild, Ralph E, and James E Newman. 1987. *Growing season characteristics and requirements in the Corn Belt*. Cooperative Extension Service, Iowa State University.
- Olmstead, Alan L, and Paul W Rhode. 2002. "The red queen and the hard reds: Productivity growth in American wheat, 1800–1940." *The Journal of Economic History* 62 (4): 929–966.
- Peng, Shu-Shi, Shilong Piao, Zhenzhong Zeng, Philippe Ciais, Liming Zhou, Laurent Z. X. Li, Ranga B. Myneni, Yi Yin, and Hui Zeng. 2014. "Afforestation in China cools local land surface temperature." *Proceedings of the National Academy of Sciences* 111 (8): 2915–2919.
- Read, Ralph A. 1958. "Great Plains shelterbelt in 1954." *Great Plains Agricultural Council*.
- Schlenker, Wolfram, and Michael J Roberts. 2006. "Nonlinear Effects of Weather on Corn Yields." *Applied Economic Perspectives and Policy* 28 (3): 391–398.
- . 2009. "Nonlinear temperature effects indicate severe damages to US crop yields under climate change." *Proceedings of the National Academy of Sciences* 106 (37): 15594–15598.
- Schulte, Lisa A, Jarad Niemi, Matthew J Helmers, Matt Liebman, J Gordon Arbuckle, David E James, Randall K Kolka, Matthew E O'Neal, Mark D Tomer, John C Tyndall, et al. 2017. "Prairie strips improve biodiversity and the delivery of multiple ecosystem services from corn–soybean croplands." *Proceedings of the National Academy of Sciences* 114 (42): 11247–11252.
- Sloat, Lindsey L, Steven J Davis, James S Gerber, Frances C Moore, Deepak K Ray, Paul C West, and Nathaniel D Mueller. 2020. "Climate adaptation by crop migration." *Nature Communications* 11 (1): 1–9.
- Smith, C, J C A Baker, and D V Spracklen. 2023. "Tropical deforestation causes large reductions in observed precipitation." *Nature* 615 (7951): 270–275.
- Snow, Meagan. 2019. "The Shelterbelt "Scheme": Radical Ecological Forestry and the Production of Climate in the Fight for the Prairie States Forestry Project." PhD diss., University of Minnesota.

- Spracklen, DV, and LJGRL Garcia-Carreras. 2015. "The impact of Amazonian deforestation on Amazon basin rainfall." *Geophysical Research Letters* 42 (21): 9546–9552.
- Taraz, Vis. 2017. "Adaptation to climate change: Historical evidence from the Indian monsoon." *Environment and Development Economics* 22 (5): 517–545.
- Taylor, Charles A. 2022. "Irrigation and Climate Change: Long-Run Adaptation and its Externalities." *Working paper*.
- "Tree Belt in West to Fight Droughts." 1934. *The New York Times*, 1.
- UNFCCC. 2022. "Nationally determined contributions under the Paris Agreement Synthesis, Fourth session Sharm el-Sheikh, 618 November 2022, report by the secretariat," <https://unfccc.int/documents/619180>.
- Yu, Chengzheng, Ruiqing Miao, and Madhu Khanna. 2021. "Maladaptation of U.S. corn and soybeans to a changing climate." *Scientific reports* 11 (1): 1–12.
- Zebiak, Stephen E, and Mark A Cane. 1987. "A model el niñ–southern oscillation." *Monthly Weather Review* 115 (10): 2262–2278.

A Appendix - For Online Publication

A.1 Downwind county definition

In order to construct our time-invariant approximate measure of how exposed county i is to winds from all Shelterbelt counties ($w_i \in [0, 1]$), we take the following steps. Let i index spillover counties, j index Shelterbelt counties and c index vertices of Shelterbelt counties. Finally, let h index the hours over the summer (June through August) for years 1981 - 2010 (e.g., $\min(h)$ is on June 1st, 1981, while $\max(h)$ is on August 31st, 2010). As discussed in the paper, we use hourly summer wind speed and direction for each Shelterbelt county for years 1981 - 2010 as spatially consistent hourly data are unavailable before the 1970s.

For each hour, we then repeat the following steps. From each vertex, v_{jc} , of each Shelterbelt county j (with total vertices V_j), we project where a particle would travel if it was blown by winds of the given direction and speed constantly for 1 day. For all unique outgoing-incoming county pairs, let $p_{ijch} = 1$ indicate if the particle from vertex v_{jc} of Shelterbelt county j intersects spillover county i for hour h . For each spillover county i , sum up all the particles originating from an outgoing county j and divide by the total number of vertices of the outgoing county.

$$p_{ijh} = \frac{\sum_c p_{ijch}}{V_j}$$

The resulting number, p_{ijh} , is the wind exposure from one county. Finally, sum up this measure from *all* Shelterbelt counties and all hours and normalize by dividing by the maximum value.

$$w_i = \frac{\sum_h \sum_j p_{ijh}}{\max \sum_h \sum_j p_{ijh}}$$

The resulting value $w_i \in [0, 1]$ is the time-invariant approximate measure of exposure to winds from the shelterbelt.

A.2 1938-1942 Wind Interpolation

We construct an alternative measure of wind exposure, based on data for 1938-1942. We use NOAA's Integrated Surface Dataset for hourly data. We first collect hourly wind data from the weather stations with wind data. We then interpolate the hourly data to a 0.5 degree grid using nearest neighbor interpolation. Figure A9 shows what the data look like before and after interpolation. We then take the same steps, described in Section A.1, in constructing an alternate wind exposure metric as with the 1981-2010 gridded wind data.

Appendix Figure A10 compares the two resulting downwind exposure metrics. Reassuringly, the measures are very similar with a correlation of 0.89.

A.3 1930-1965 climate data construction

We build our main weather data from daily station data using methodology inspired by Schlenker and Roberts (2006). We use NOAA's Global Historical Climatology Network daily (GHCNd) data to create a balanced panel of stations with availability between 1930 and 1965. We take the following steps to construct our county-level daily data.

1. Start with precipitation and temperature stations from the GHCNd stations that are available for 1930 through 1965 (2,001 and 1,445 precipitation and temperature stations, respectively).
2. Select a constant set of stations based on availability. Keep stations with less than 5% missing observations between 1930 and 1965 (1,099 and 750 precipitation and temperature stations, respectively).
3. Fill in missing observations for this set of constant stations.
 - a. For each station, S_i , find the 10 closest stations in the data.
 - b. For each of the 10 nearby stations, calculate the percentile of the daily precipitation and maximum and minimum temperatures readings for each day, based on the entire available distribution of weather measures at the appropriate station.
 - c. For each missing observation for station S_i , calculate the average percentile reading of the 10 closest stations (e.g., 71st percentile).
 - d. Then, fill in the missing observation using the corresponding value from the distribution of S_i (e.g., if the 71st percentile corresponds to 20mm of precipitation at station S_i , the missing value will be filled in with 20mm).
4. Calculate degree days at each station.
5. Interpolate all variables to a 0.1 degree grid.
6. Average gridded values at the county level.

A.4 Decomposition of yield effects

We estimate the direct (mechanical) effect of the Shelterbelt-induced climate change on yields, in the downwind neighbor counties. We do so in three steps.

For the first step, we use the canonical Schlenker and Roberts (2009) piece-wise linear model to estimate the weather-yield relationship on counties non affected by the Shelterbelt project. Specifically, focusing on the non-downwind (other) neighboring and control counties, we use year-to-year variation in weather within counties and estimate the model for the period post-1942:

$$y_{it} = \mu + \delta_1 DD10_{it} + \delta_2 DD29_{it} + \delta_3 DD39_{it} + \theta_1 precip_{it} + \theta_2 precip_{it}^2 + d_i + z_{it} + \nu_{it} \quad (7)$$

where y_{it} are annual log yields, DDX_{it} are average summer monthly degree days above $X^{\circ}\text{C}$, $precip_{it}$ is average summer monthly precipitation, d_i are county fixed effects, and z_{it} are quadratic time trends for each state. Appendix Table A5 shows the results from this estimation. Consistent with the original results from Schlenker and Roberts 2009, 10°C degree days and precipitation have a positive impact on yields, while harmful degree days above 29°C and 39°C have negative effects on yields.

In the second step, we estimate treatment effects for each variable entering Equation 7 above using our main difference-in-differences model. Table 4, Columns (1)-(5) show the results for each variable of interest. We then subtract the estimated treatment effects to obtain the weather absent Shelterbelt planting: $w_{1i} = w_{0i} - TE$.

In the third step, we use the estimated Equation from the first step and realized weather (w_{0i}) to predict yields for each county (y_{0i}). We average post-treatment (1942 to 1965) weather variables and predict average post-period log yields (\hat{y}_{0i}) for downwind neighbor counties. We then repeat these steps, except replacing average realized weather (w_{0i}) with average weather that would have taken place absent Shelterbelt planting (w_{1i}). We predict yields using w_{1i} to obtain counterfactual yields \hat{y}_{1i} . Finally, we compute the average treatment effects on log yields using

$$ATE_{mecha} = \frac{1}{N} \sum_{i=1}^N (\hat{y}_{1i} - \hat{y}_{0i})$$

The expected mechanical effect of climate change on yields is shown in Column (6) of Table ??.

A.5 Station-level analysis

We repeat our main analysis at a hyperlocal level, using individual weather station data along with the shapefile of the exact location and area of surviving Shelterbelt plantings (Snow 2019).

We start with weather station data from NOAA’s Global Historical Climatology Network daily (GHCNd) data. We use the same procedure as for the construction of our main climate data described in Appendix Section A.3. However, we use 1910 - 1965 precipitation and temperature data and stop before interpolating to a grid. The procedure results in station-level daily data, which we average to monthly values as before. We keep GHCNd stations within the Shelterbelt (as defined by our Shelterbelt treatment dummy). This corresponds to 79 precipitation and 51 temperature stations.

Using the Shelterbelt shapefile from Snow (2019), we calculate the area of tree planting within a 25km radius of each station. We then estimate a version of our main difference-in-differences Equation (Equation 1)

$$y_{st} = \beta_{LOC}(AA_s \times P_t) + \xi_t + \rho_s + \epsilon_{st} \quad (8)$$

where y_{st} is the outcome of interest at the station-year level, AA_s is the area afforested within 25km of the station (in 1000 acres), and P_t is a dummy variable equal to one for years after 1942. We include year (ξ_t) and station (ρ_s) fixed effects. β_{LOC} is the hyperlocal effect of planting an addition 1000 acres of trees for stations located in the Shelterbelt region.

Since we find significant spillover effects in our main analysis and these forces may impact our selected stations, we expect that the results from the hyperlocal analysis may be lower in magnitude than the true effect from local tree planting. Nevertheless, we find that stations with more nearby afforestation recorded higher precipitation and lower temperatures in the decades after the Shelterbelt project.

Appendix Table A16 shows the results. The results for precipitation are statistically significant and imply that planting 1000 additional acres of trees in the vicinity of a station lead to 1.2% more post-treatment summer precipitation. Average and extreme temperatures also decreased, though these estimates are less precise. These findings show that the change in climate due to tree planting holds at the local level.

A.6 Synthetic difference-in-differences

To address possible concerns with the parallel trends assumption, we repeat our difference-in-differences with binary treatment variables analyses using a synthetic difference-in-differences approach. Since the synthetic difference-in-differences creates parallel pre-trends across treated and control units by design, the method also addresses concerns regarding differential exposure to the Dust Bowl.

The synthetic difference-in-differences method, described by Arkhangelsky et al. (2021), combines features of the synthetic control and difference-in-differences methods. The synthetic difference-in-differences method weakens reliance on parallel trends by reweighing and matching pre-exposure trends. The method then uses the resulting weights in a two-way fixed effects regressions to estimate the average causal effect of exposure to the treatment. We use the synthetic difference-in-differences method to compare treated Shelterbelt counties to a synthetic control and to compare downwind and other neighbor counties to separate synthetic controls. Possible contributors to the synthetic controls are counties from the pure control group and from outside our study sample. They all come from areas in the Northern and Southern Great Plains. Specifically, we use counties with centroids between 108°West and 88°West.

Formally, consider a balanced panel with N total counties (e.g., Shelterbelt and pool of untreated counties, or spillover and pool of untreated counties) indexed by i and U periods indexed by t . Like before, treatment exposure is denoted by $(T_i \times P_t) \in \{0, 1\}$, where T_i indicates treatment status and P_t treatment timing. The synthetic differences method finds weights $\hat{\omega}^{sdid}$ and $\hat{\lambda}^{sdid}$ to align pre-exposure trends in treated and unexposed counties as well as to balance pre-exposure periods with post-exposure ones. These weights are used in the following two-way fixed effects regression

$$(\hat{\tau}^{sdid}, \hat{\mu}, \hat{\alpha}, \hat{\beta}) = \arg \min \left\{ \sum_{i=1}^N \sum_{t=1}^U (y_{it} - \mu - \alpha_i - \beta_t - (T_i \times P_t)\tau)^2 \hat{\omega}_i^{sdid} \hat{\lambda}_t^{sdid} \right\}. \quad (9)$$

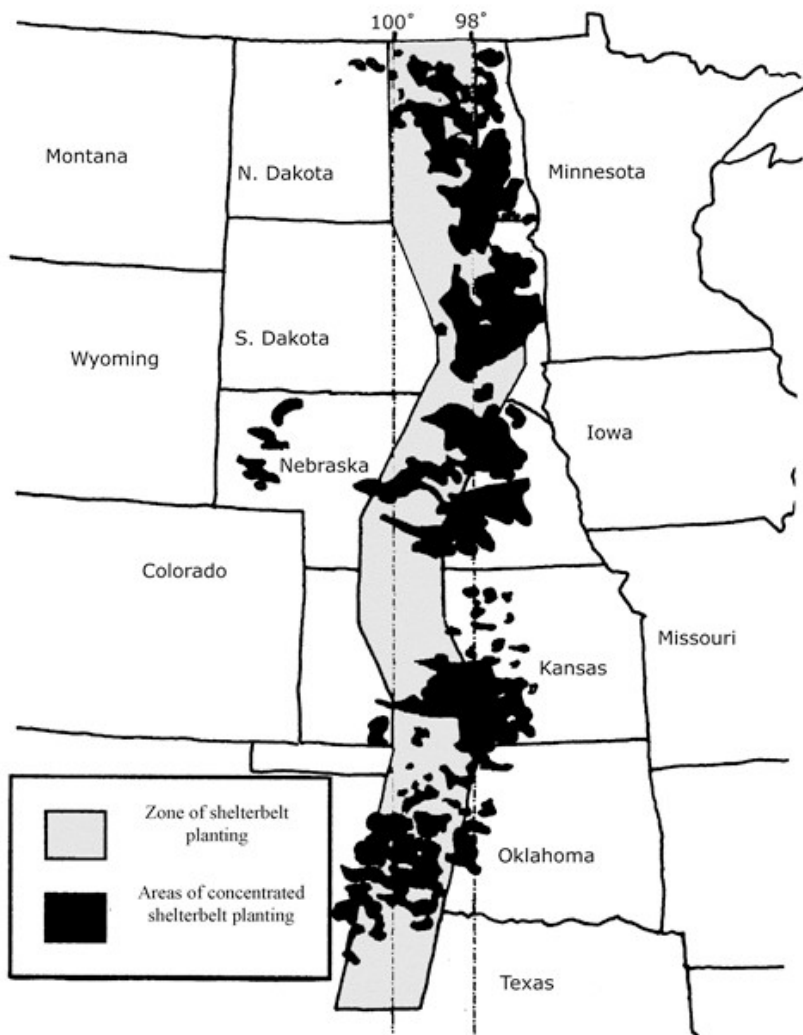
The difference between Equation 9 and the standard two-way fixed effects regression described in Equation 5 is only the addition of the unit and time weights ($\hat{\omega}^{sdid}$ and $\hat{\lambda}^{sdid}$) (Arkhangelsky et al. 2021).

Appendix Table A8 shows the results for climate outcomes. The results for rainfall are slightly higher in magnitude, while the results for the various temperature measures are slightly lower in magnitude. Nonetheless the overall results are consistent with our main difference-in-differences estimates. Appendix Table A9 presents results for corn yields, which

are slightly lower in magnitude, but generally in line with our main results. Appendix Figures A17 and A18 shows the trends in outcomes and corresponding treatment effects for Shelterbelt and downwind neighbor counties compared to the synthetic controls for climate and economic outcomes.

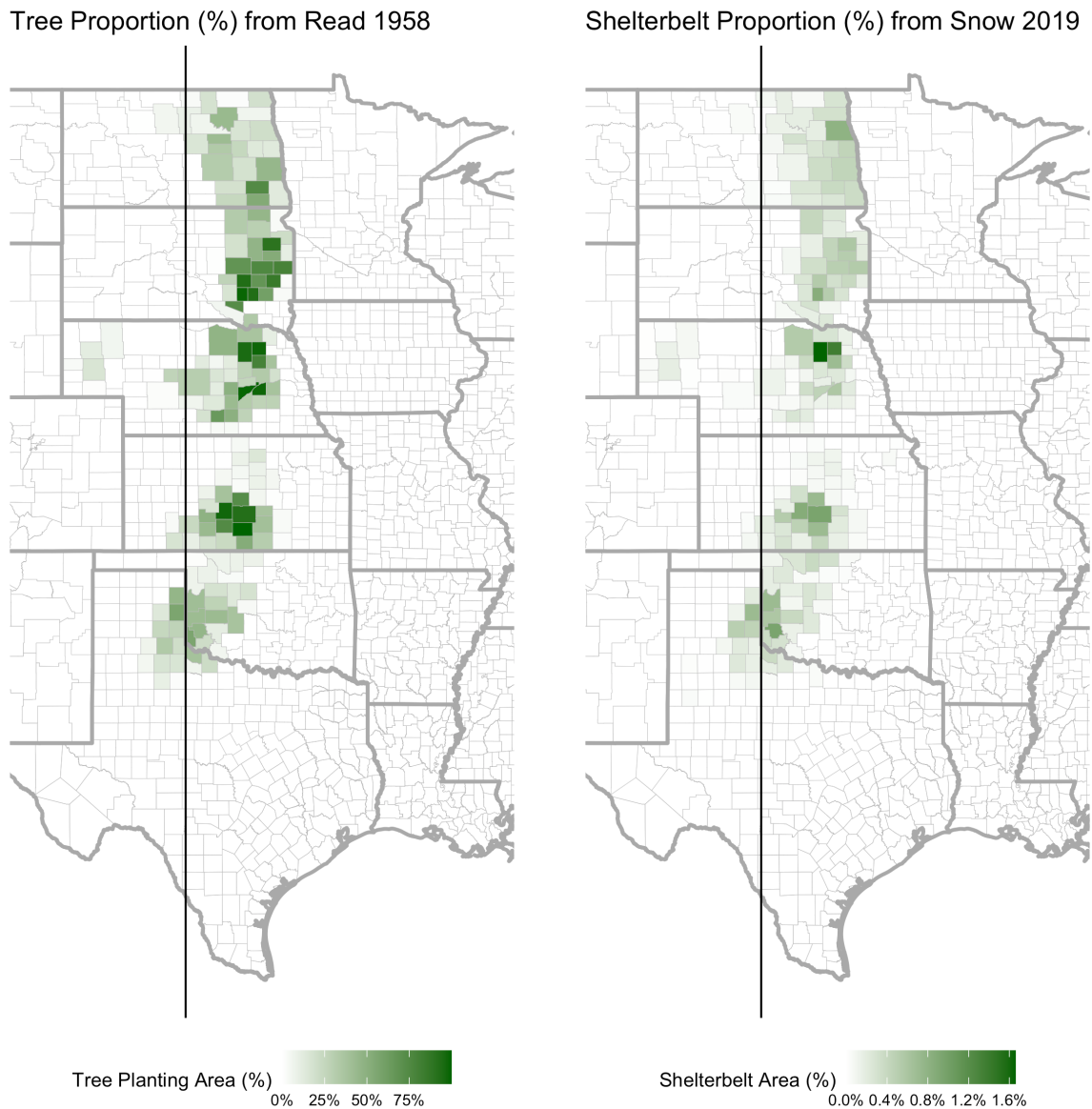
Appendix Figures

Figure A1: Shelterbelt planned area and realized concentrated planning



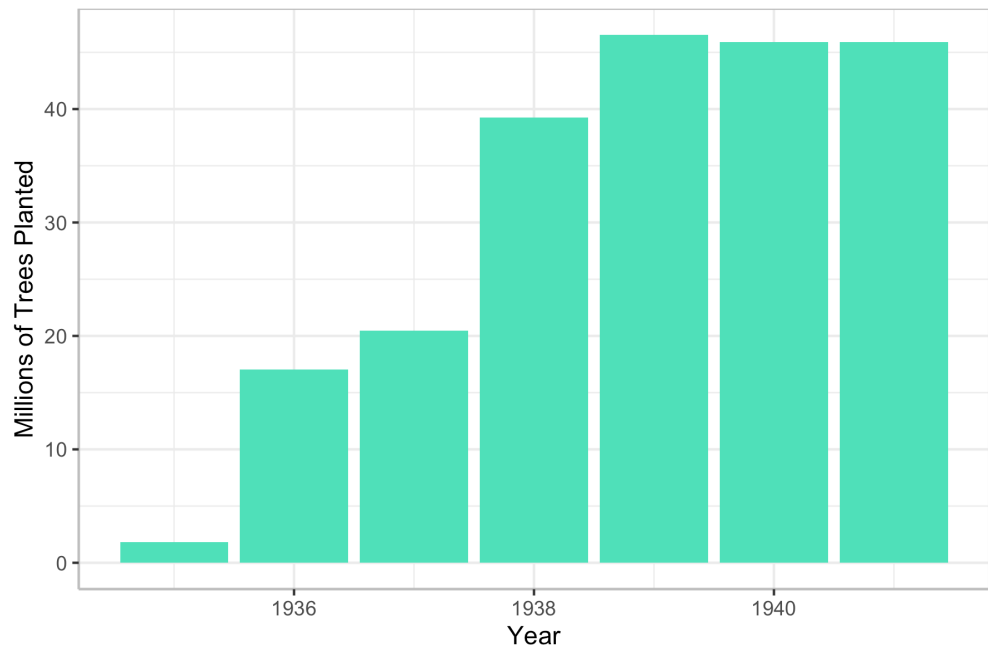
Notes: Map shows planned zone of Shelterbelt planting and areas of concentrated Shelterbelt planting according to Read 1958. Our Shelterbelt definition is based on county areas covered by the areas of concentrated tree planting.

Figure A2: Shelterbelt measures



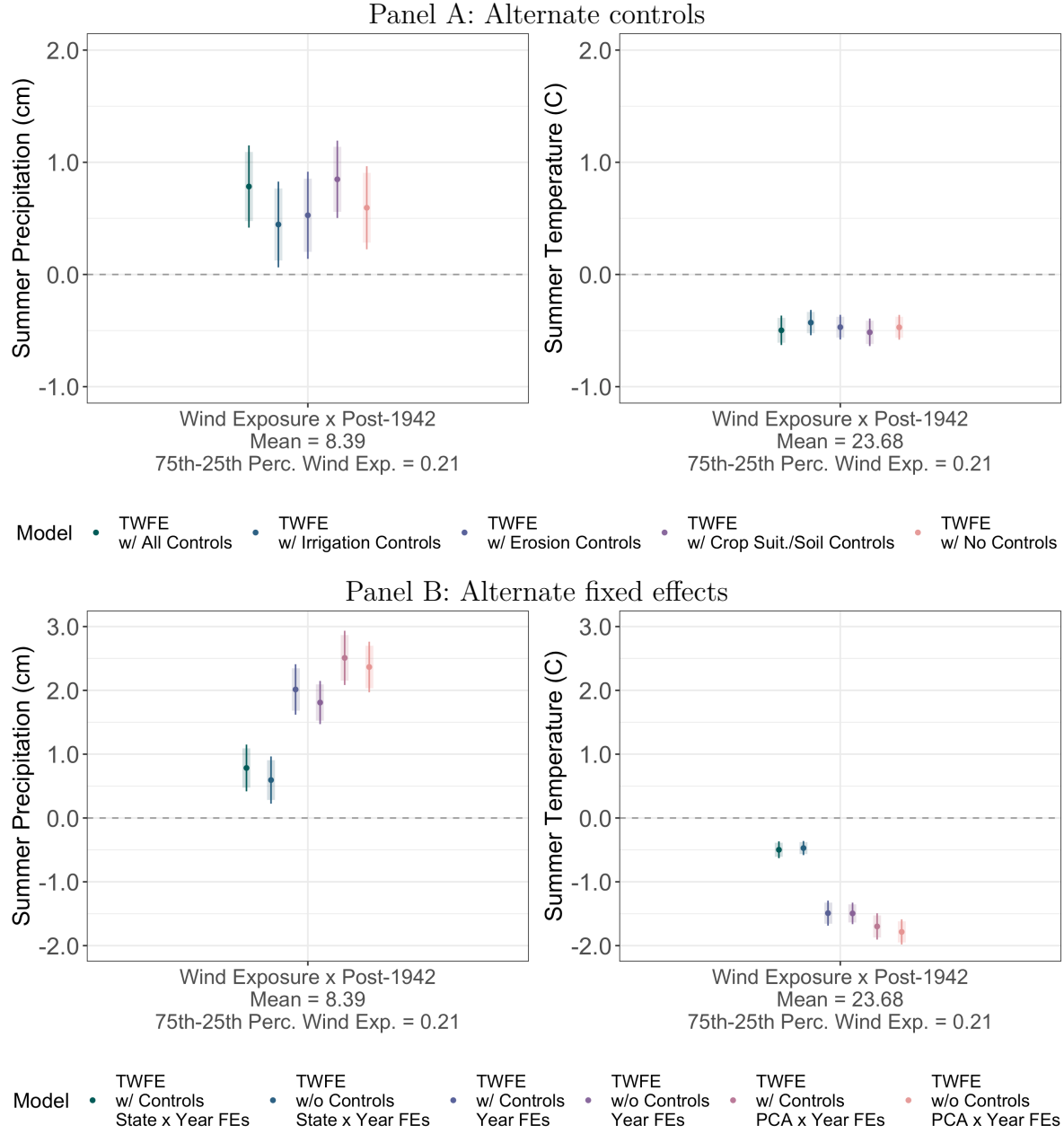
Notes: Figure compares our main measure of Shelterbelt treatment from Read (1958) and an alternate measure from Snow (2019) used for robustness checks. The two measures are similar (correlation 0.86).

Figure A3: Shelterbelt tree planting over time



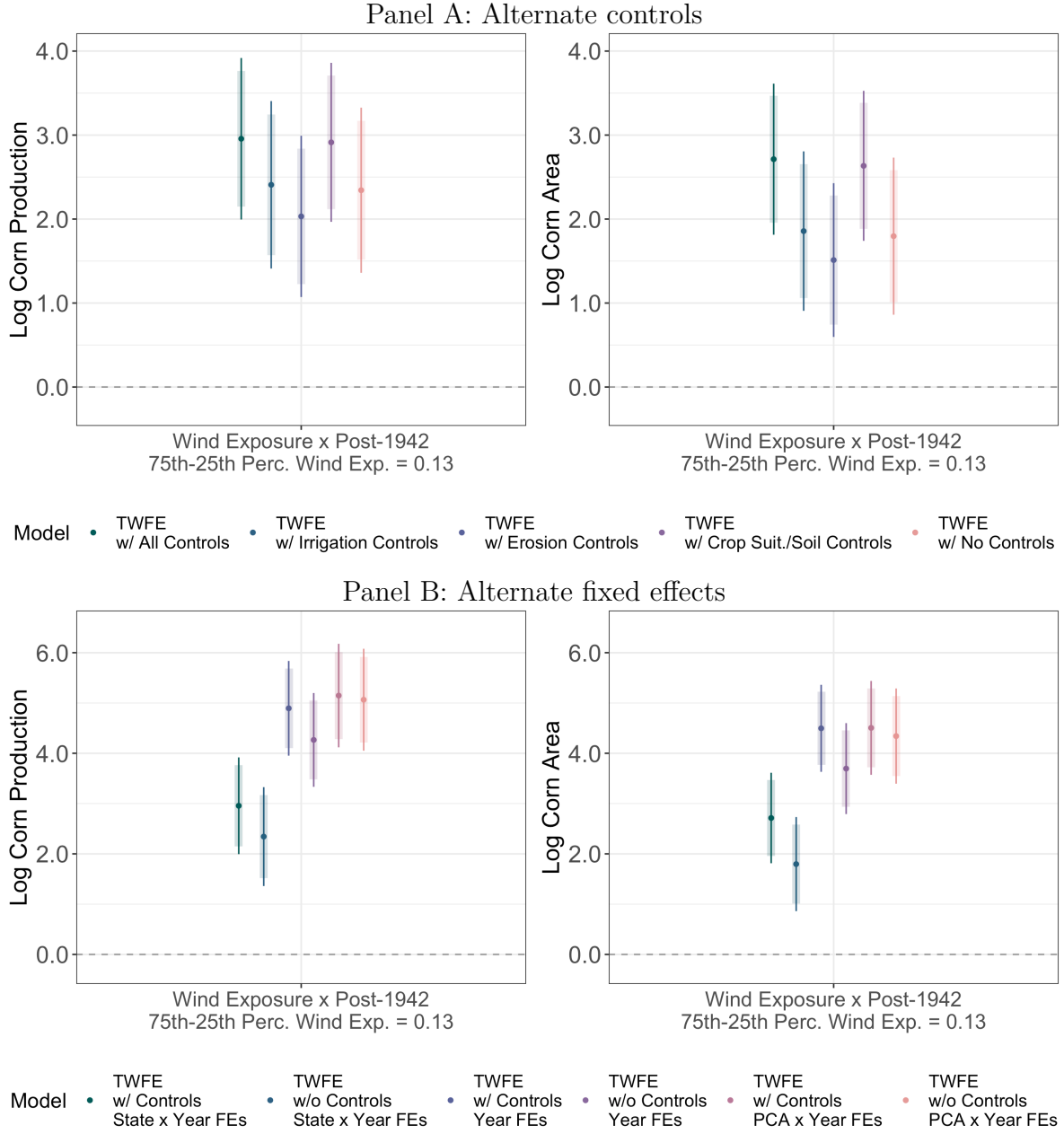
Notes: Figure plots the number of trees planted in each year of the Shelterbelt project implementation. Figures for 1940 and 1941 are estimates based on overall count of trees planted.

Figure A4: Climate results robustness



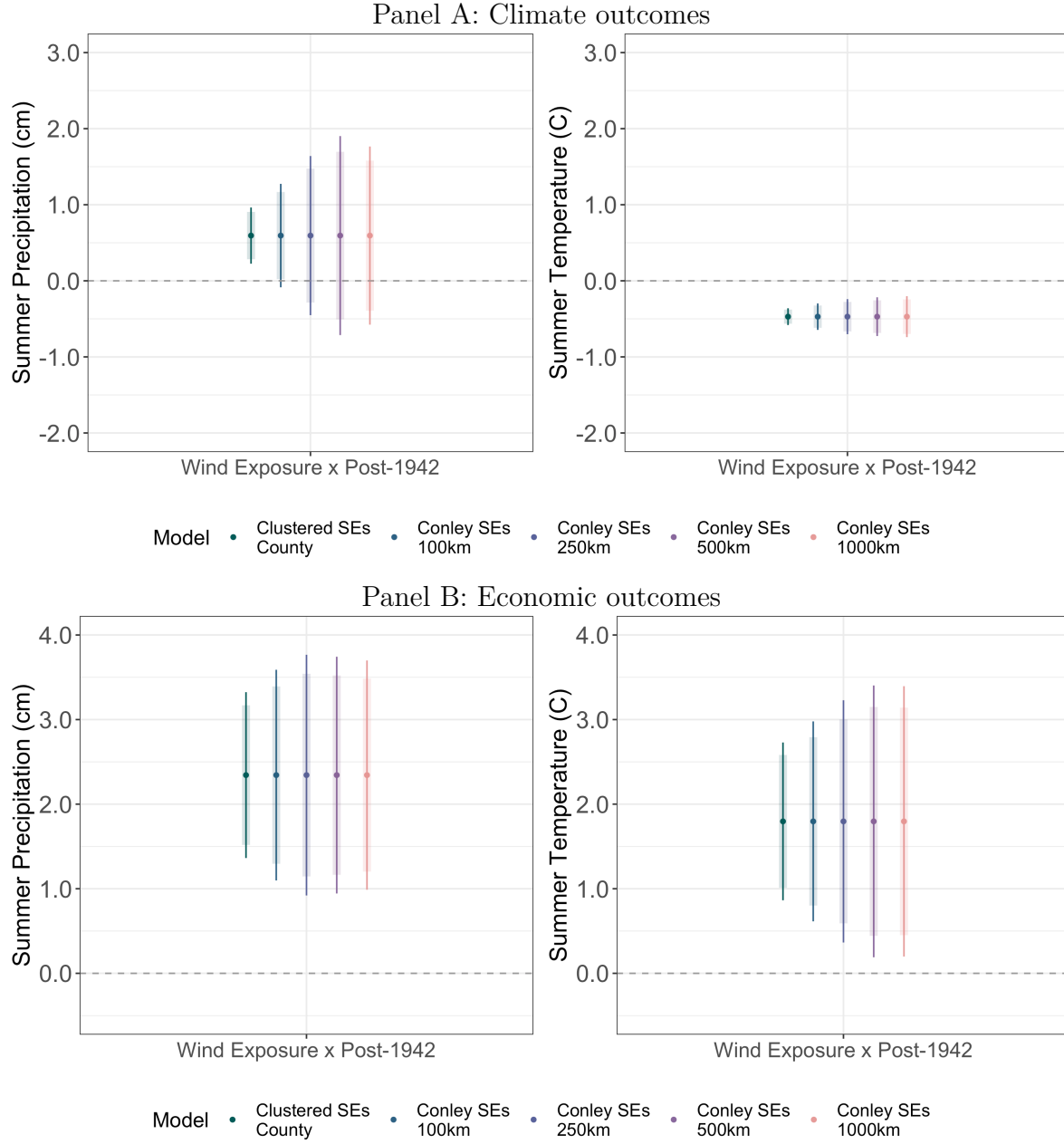
Notes: Figures plot coefficient estimates and 95% (thin line) and 90% (thick line) confidence intervals for mean summer precipitation and mean summer temperatures. In Panel A, we show robustness across five versions of estimating Equation 1 with various controls. In the first, we show our main results with all controls. Next, we include only the county area irrigated in 1935, Dust Bowl erosion measures, and crop suitability and soil type controls. Finally, we drop all controls. In Panel B, we show robustness across six specifications (based on Equation 1) with various fixed effects. In the first two, we show our main results with state-by-year (and county) fixed effects, with and without controls. Next, we include only year (and county) fixed effects. Finally, we include principal component quadrant by year fixed effects. To create these quadrants, we perform principal component analysis using county-level data on maize and wheat crop suitability, ustolls share of county area, Ogallala share of county area, Great Plains ecoregion share of county area, erosion during the Dust Bowl, share of the county area irrigated in 1935, average elevation and ruggedness, and average precipitation, maximum and minimum temperatures. We then create quintiles based on the main principal component.

Figure A5: Corn production and area results robustness



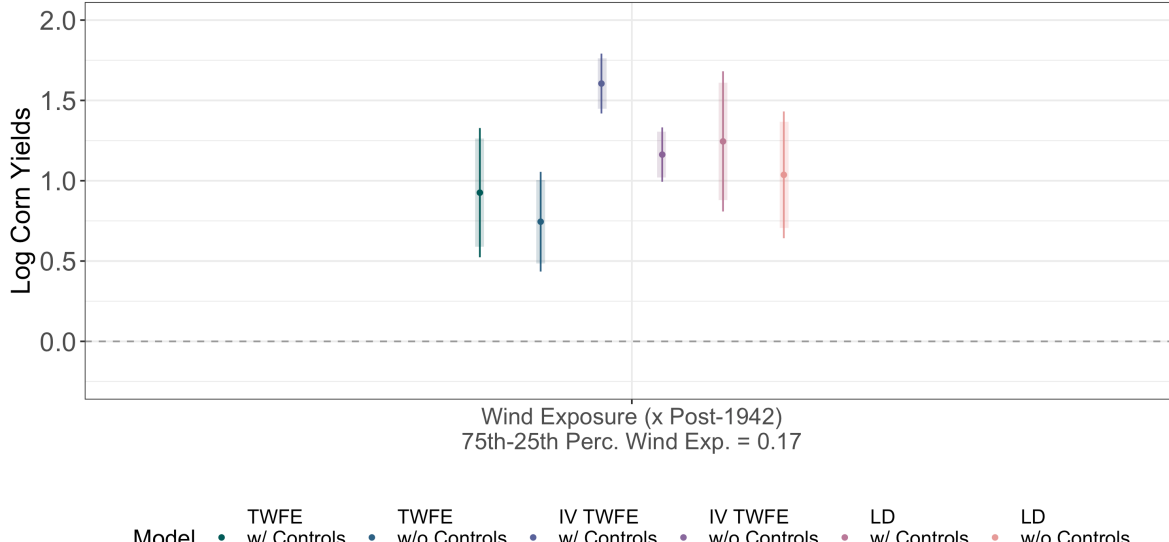
Notes: Figures plot coefficient estimates and 95%(thin line) and 90% (thick line) confidence intervals for mean summer precipitation and mean summer temperatures. In Panel A, we show robustness to five specifications (based on Equation 1) with various controls. In the first, we show our main results with all controls. Next, we include only the county area irrigated in 1935, Dust Bowl erosion measures, and crop suitability and soil type controls. Finally, we drop all controls. In Panel B, we do the same with six specifications with various fixed effects. In the first two, we show our main results with state-by-year (and county) fixed effects, with and without controls. Next, we include only year (and county) fixed effects. Finally, we include principal component quadrant by year fixed effects. To create these quadrants, we perform principal component analysis using county-level data on maize and wheat crop suitability, ustolls share of county area, Ogallala share of county area, Great Plains ecoregion share of county area, erosion during the Dust Bowl, share of the county area irrigated in 1935, average elevation and ruggedness, and average precipitation, maximum and minimum temperatures. We then create quintiles based on the main principal component.

Figure A6: Robustness to Conley standard errors



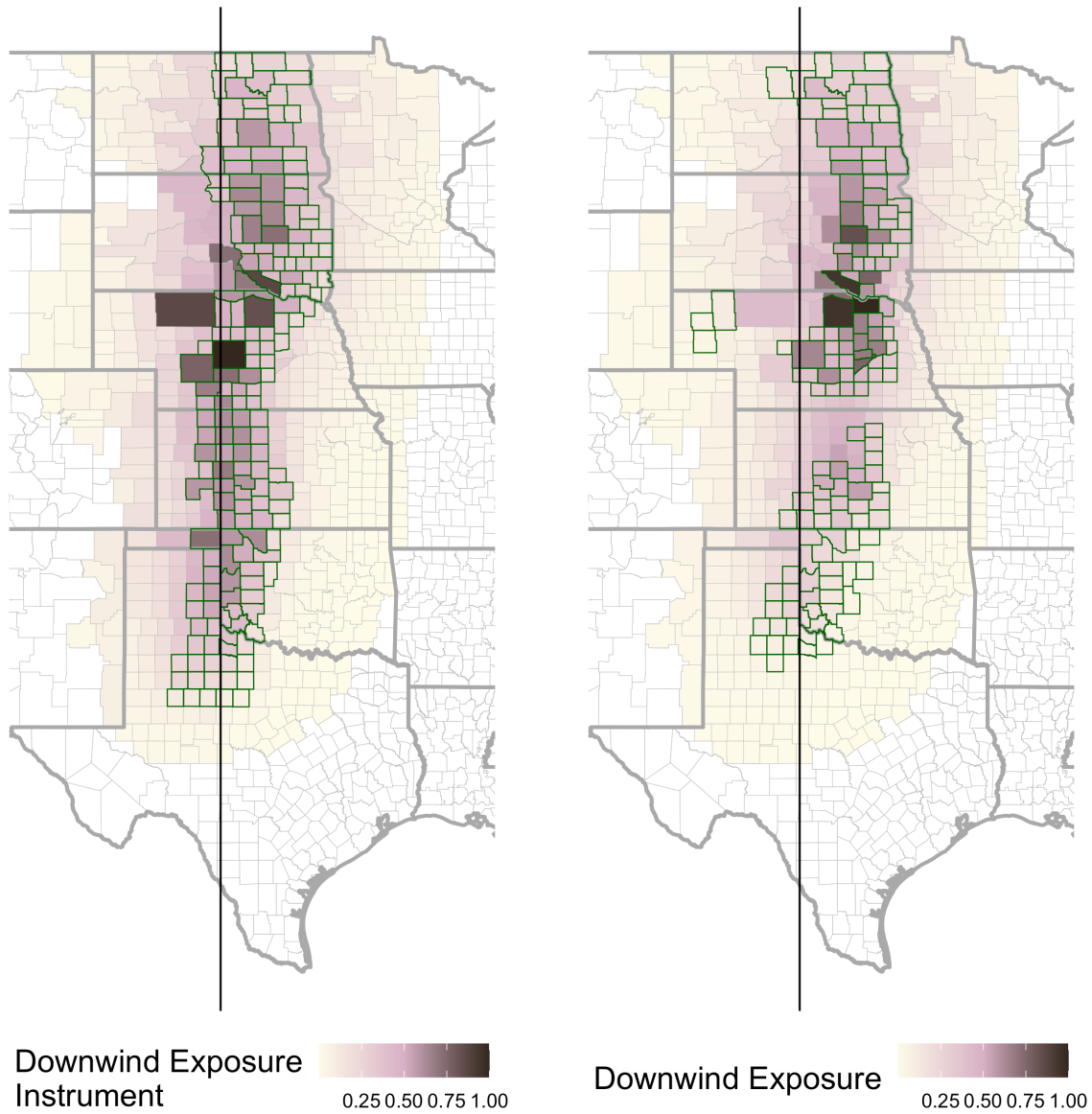
Notes: Figures plot coefficient estimates and 95%(thin line) and 90% (thick line) confidence intervals using for climate outcomes (Panel A) and economic outcomes (Panel B). In the first version of each regressions, we show our main results without controls (Equation 1), using clustered standard errors at the county level. We then repeat the same regression using Conley standard errors are various distance cutoffs.

Figure A7: Corn yield results robustness to alternative NASS survey data



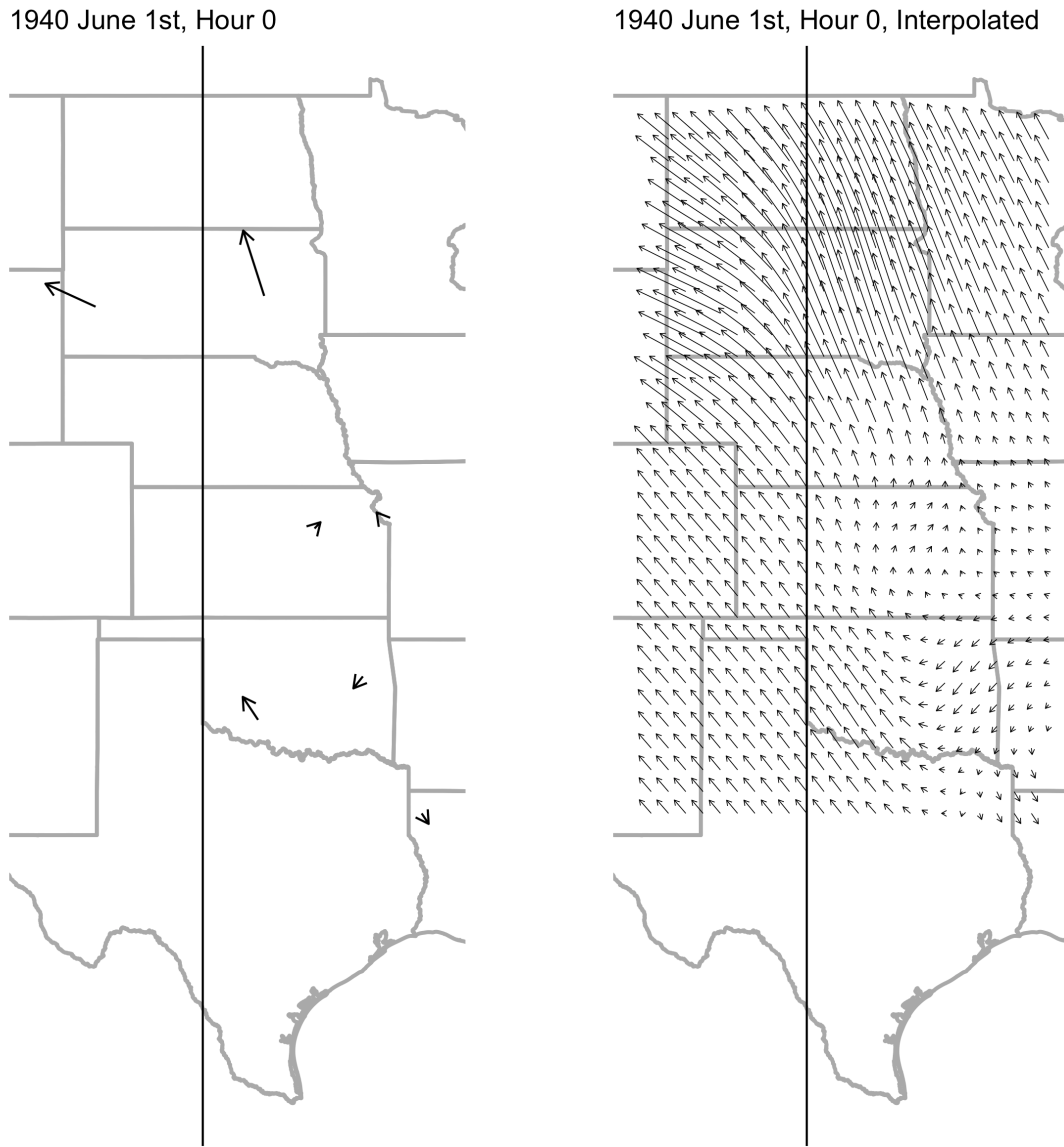
Notes: Figures plot coefficient estimates and 95%(thin line) and 90% (thick line) confidence intervals from three different models: TWFE (Equation 1), instrumental variables TWFE (Equation 3), long differences (LD) (Equation 4) each with and without controls. Dependent variable is log corn yields from the NASS annual surveys, for 230 counties, a subset of counties in our area of interest. Main independent variable is wind exposure (w_i), which measures approximate exposure to winds from afforested areas, interacted by a post-treatment dummy for the TWFE models. “75th-25th Perc Wind Exp” shows the difference between the 75th and 25th percentile of the continuous wind exposure measure. Time-invariant controls include county-level crop suitability, soil characteristics, Dust Bowl erosion measures, and 1935 irrigation intensity. County and state-by-year (or state, for LD) FE included.

Figure A8: Wind exposure and wind exposure instrument



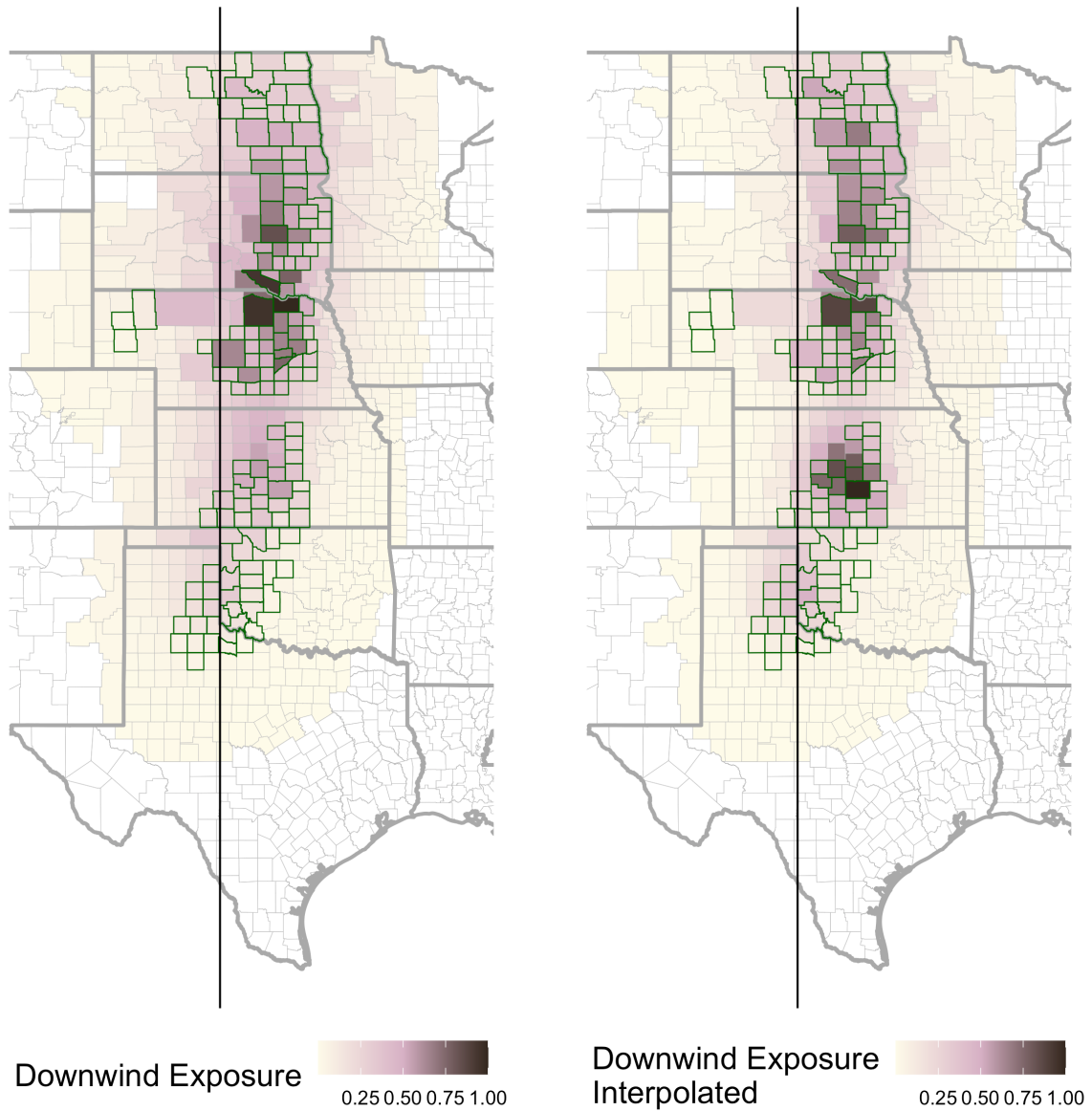
Notes: Left panel shows the instrument for the continuous wind exposure measure constructed based on the planned 100-mile Shelterbelt zone. Right panel shows the final continuous wind exposure measure based on realized Shelterbelt planting. Dark green outlines show planned and realized Shelterbelt counties.

Figure A9: Wind interpolation example



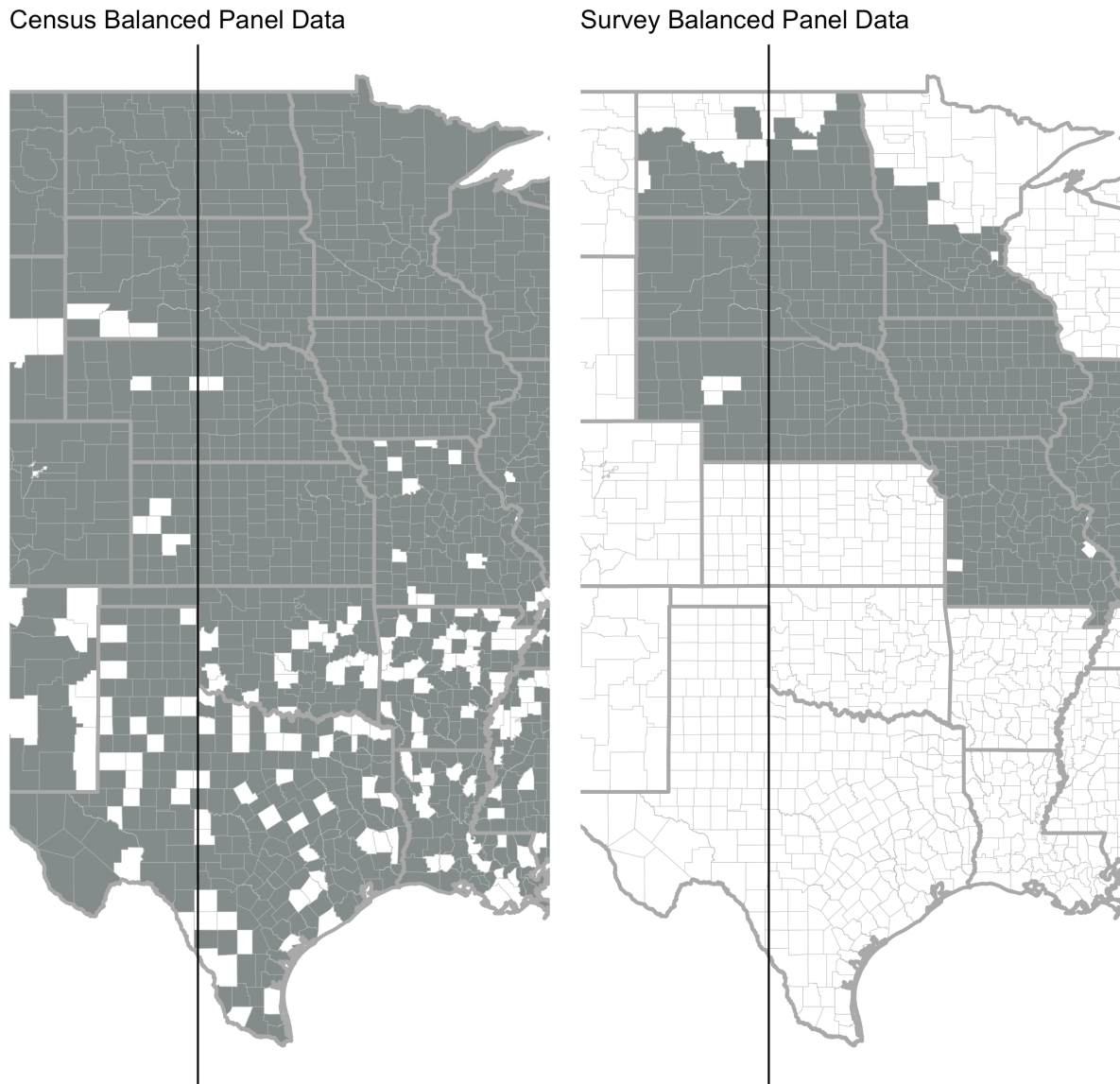
Notes: Figure shows sparse 1938 - 1942 wind station data interpolation for a given hour. The left panel shows wind direction and speeds for available stations in the US Midwest on 1940 June 1st, midnight to 1am. The right panel shows the wind data interpolated to a 0.5 degree grid.

Figure A10: Wind exposure measures



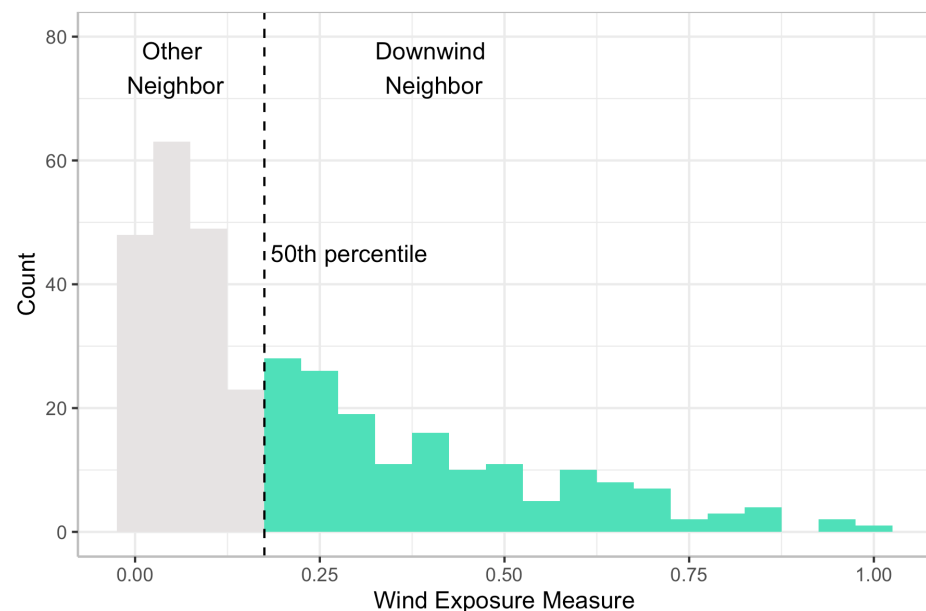
Notes: Maps show two alternate wind exposure metrics. Counties with green borders are treated Shelterbelt counties while shading shows continuous wind exposure measure. The left panel shows our main wind exposure measure based on 1981 - 2010 long-term average winds, while the right panel shows the same measure but using interpolated 1938 - 1942 wind station data. Reassuringly, the two measures are very similar (correlation 0.92).

Figure A11: Agricultural survey and census data



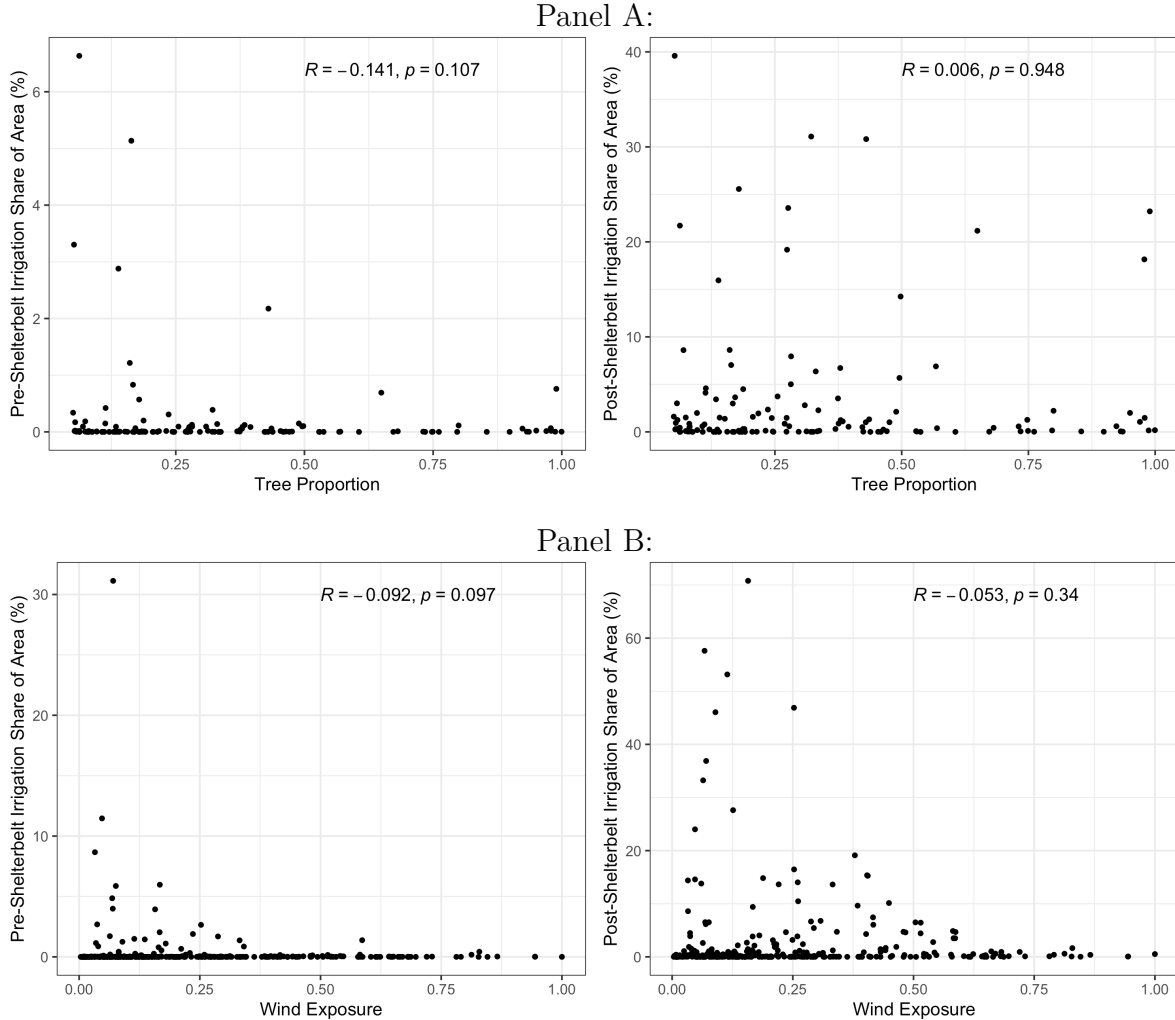
Notes: Figure shows counties for which we have corn yield observations from the agricultural census and surveys for every time period between 1930 and 1965.

Figure A12: Shelterbelt neighbor wind exposure



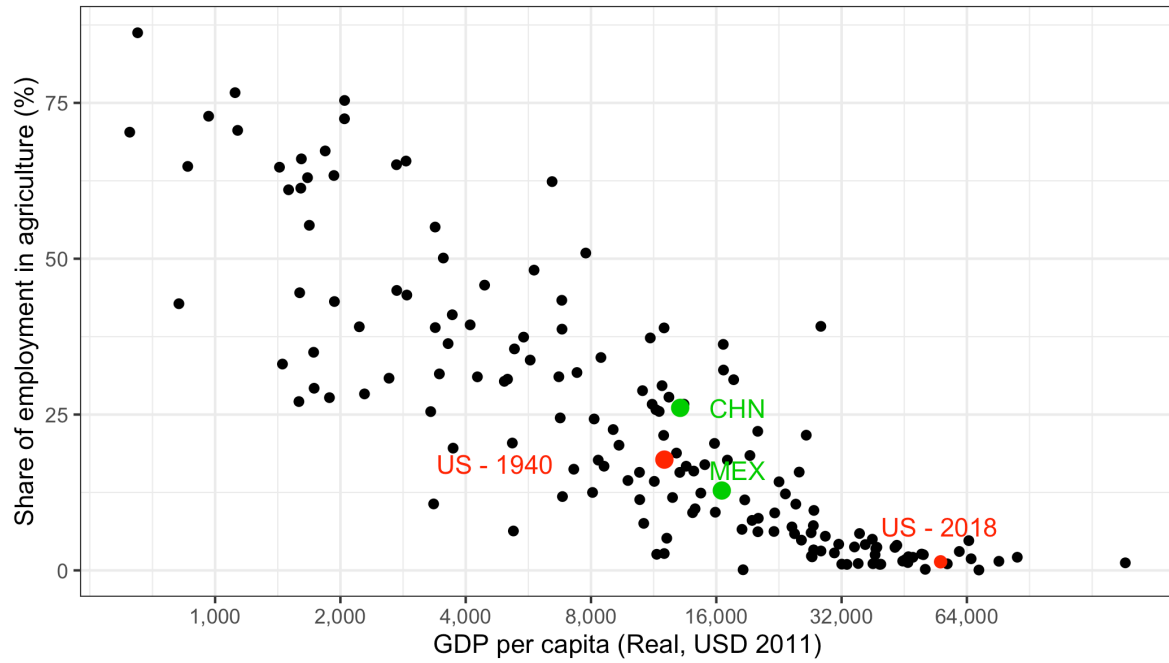
Notes: Figure shows histogram of the wind exposure measure for counties within 200km of afforested areas. Counties with wind exposure above the median measure are classified as downwind neighbor counties, while the rest are classified as other neighbors.

Figure A13: Irrigation and Shelterbelt planting



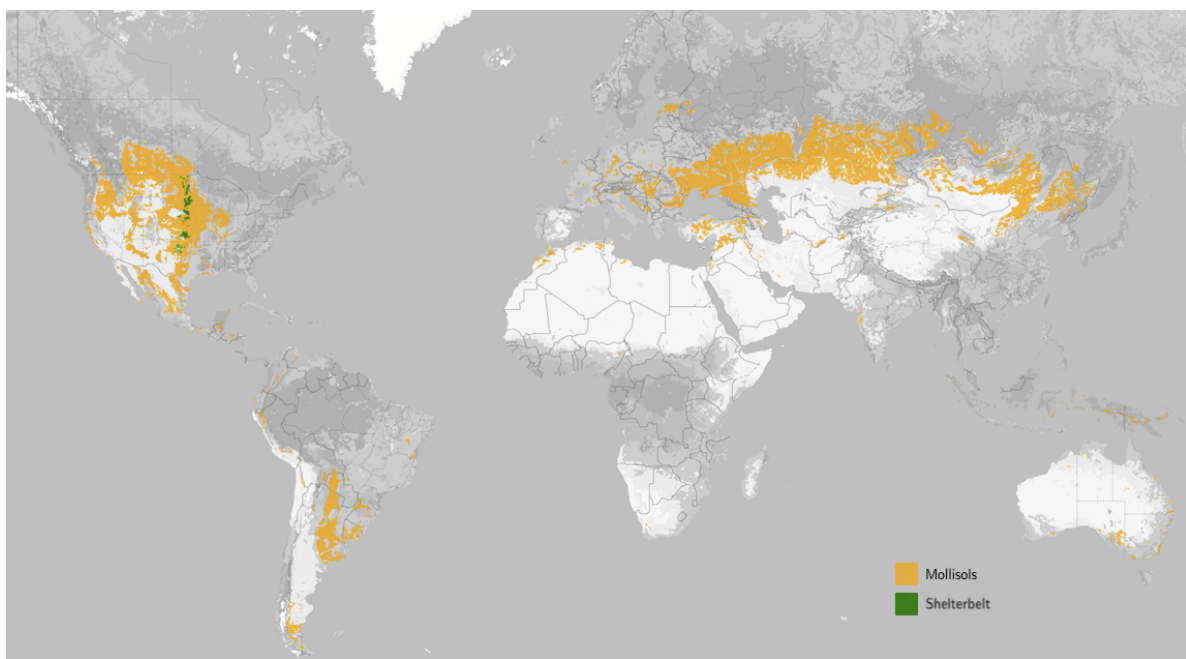
Notes: Panel A shows scatterplots of concentrated Shelterbelt planting as a share of county area on the x axis and irrigated land as a share of county area on the y axis. Panel B shows wind exposure measure from the Shelterbelts on the x axis and irrigated land as a share of county area on the y axis. Left plots shows irrigation prior to the Shelterbelt project (1935), while the right plots shows irrigation post afforestation (1959).

Figure A14: United States in 1940, compared to countries in 2018



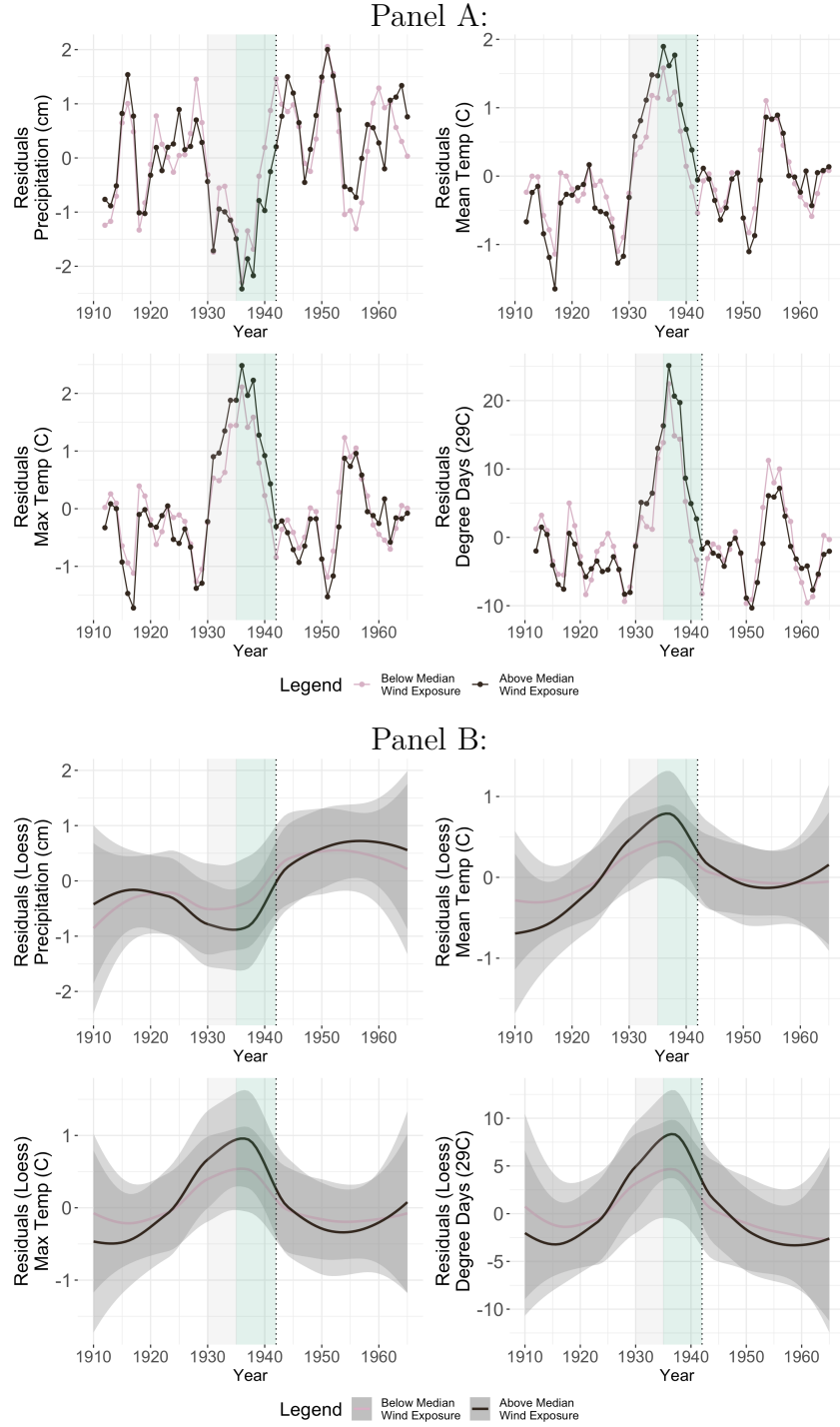
Notes: GDP per capita from the Maddison Project Database (2018 and 1940). Share of employment in agriculture from the US Census (1940, IPUMS) and the World Development Indicators (2018, WB).

Figure A15: Distribution of Mollisols



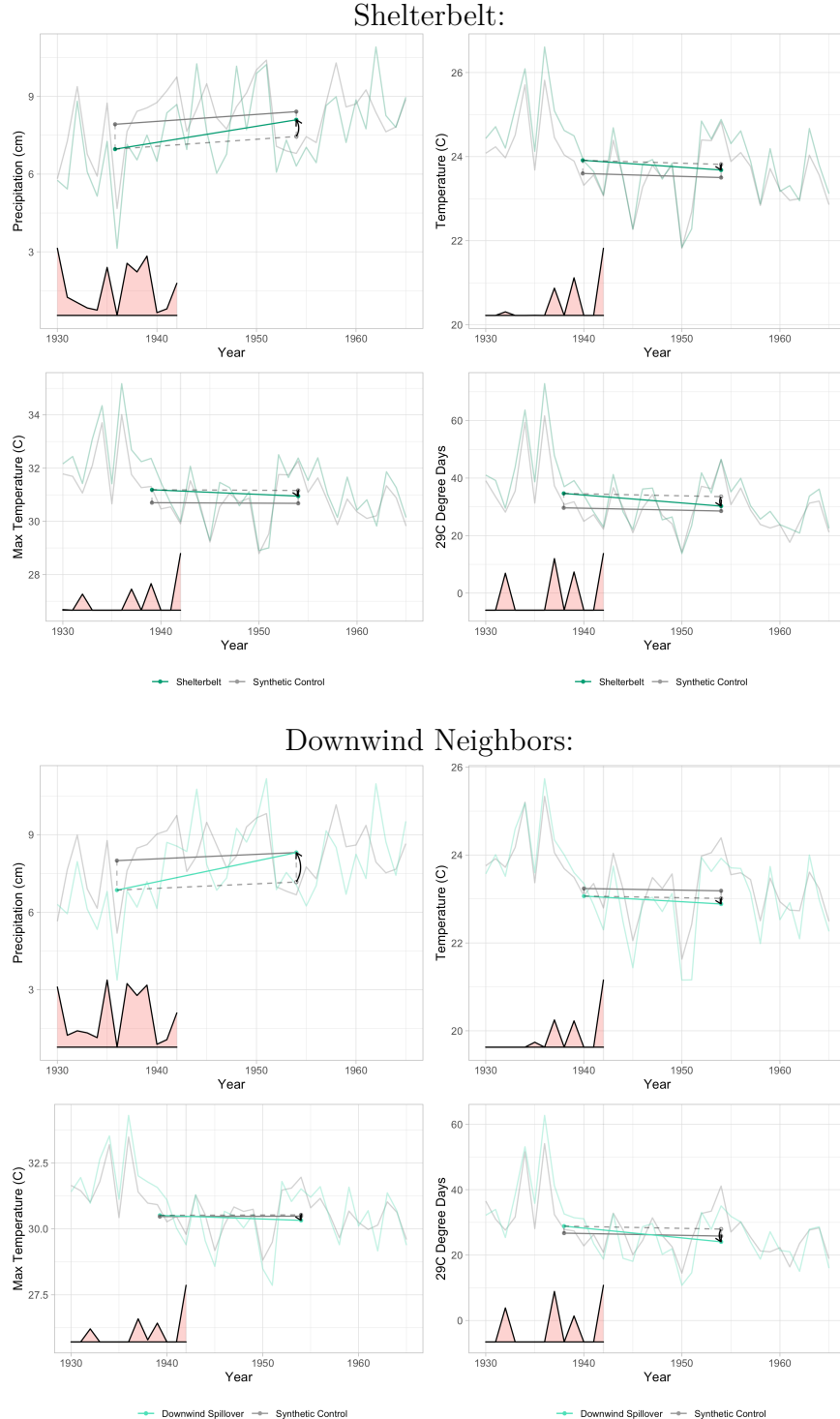
Notes: Soil map derived from USDA NRCS.

Figure A16: Trends in climate outcomes for affected and control counties, 1910 - 1965



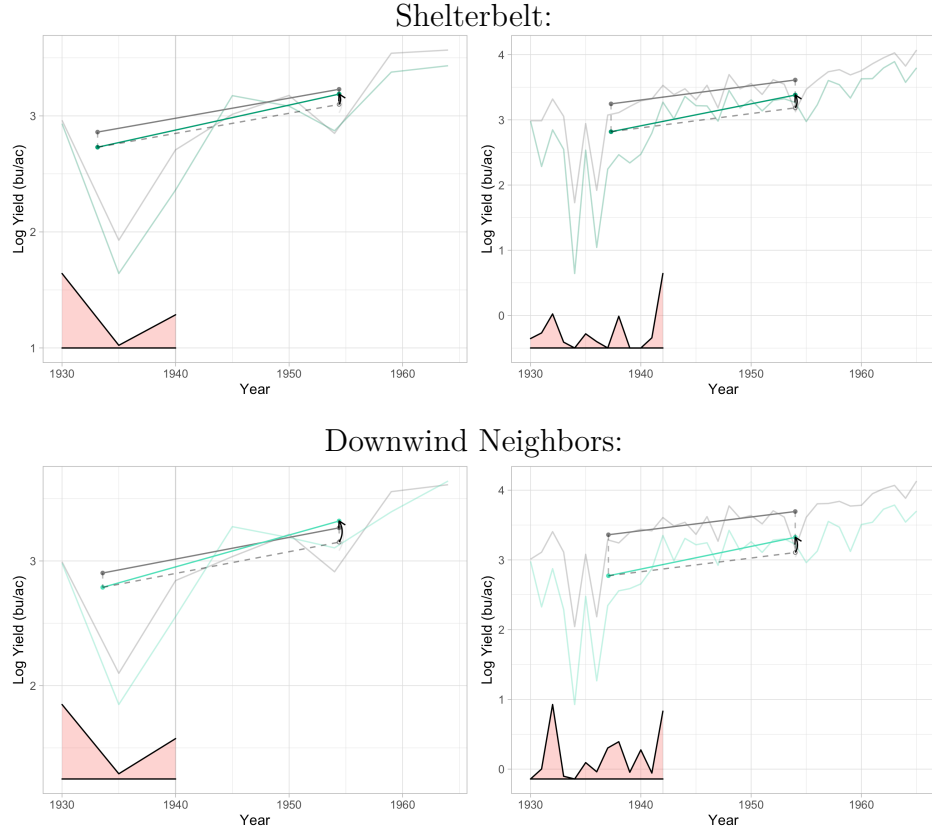
Notes: Figures plot average residuals for 1910-1965, for counties above and below the median wind exposure measure. Gray shaded area shows pure baseline period (without tree planting), green shaded area shows Shelterbelt project years. Panel A shows climate outcomes of summer precipitation, mean/maximum summer temperatures, and 29C degree days, with 3-year rolling averages used due to high variation in annual weather outcomes. Residuals shown after controlling for state and county fixed effects. Panel B shows same outcomes, but a LOESS best fit line to show trends.

Figure A17: Climate synthetic difference-in-differences graphs



Notes: Figure shows climate synthetic difference-in-differences results graphically. Shelterbelt (top panel) and downwind neighbor (bottom panel) precipitation and temperature trends are plotted along with their respective synthetic controls trends; weights used to average pretreatment time periods are shown at the bottom of the graphs in red. The synthetic difference-in-differences method emphasizes periods that are on average more similar to treated periods, therefore the synthetic control trend (gray) is further adjusted using the weights shown at the bottom of the graphs. The estimated effect is indicated by the arrow.

Figure A18: Corn yields synthetic difference-in-differences graphs



Notes: Figure shows corn yield synthetic difference-in-difference results graphically. Shelterbelt (top panel) and downwind neighbor (bottom panel) yields from the census (left panel) and agricultural surveys (right panel) are plotted along with their respective synthetic control trends; weights used to average pretreatment time periods are shown at the bottom of the graphs in red. The synthetic difference-in-differences method emphasizes periods that are on average more similar to treated periods, therefore the synthetic control trend (gray) is further adjusted using the weights shown at the bottom of the graphs. The estimated effect is indicated by the arrow.

Appendix Tables

Table A1: Impact of Great Plains Shelterbelt on Jun-Aug county climate, 1930 to 1965
(Exluding directly afforested counties)

	<i>Dependent variable:</i>			
	Precipitation (cm)	Mean Temp (C)	Max Temp (C)	Degree Days (29C)
	(1)	(2)	(3)	(4)
Wind Exposure:Post 1942	1.666*** (0.290) [0.000]	-0.846*** (0.096) [0.000]	-1.292*** (0.140) [0.000]	-14.532*** (1.330) [0.000]
Mean	8.47	23.68	30.84	28.40
Std.Dev.	3.64	3.03	3.15	22.22
75th-25th Perc. Wind Exp	0.12	0.12	0.12	0.12
Observations	16,776	16,776	16,776	16,776

Notes: Standard errors clustered at the county level shown in parentheses; p-values shown in brackets (*p<0.1; **p<0.05; ***p<0.01). Table shows results for estimating Equation 1 for 539 counties, with centroids within 300km of the centroids of Shelterbelt counties, dropping directly afforested counties. Dependent variables are June - August averages. Main independent variable is wind exposure (w_i), which measures approximate exposure to winds from afforested areas, interacted by a post-treatment dummy. “75th-25th Perc Wind Exp” shows the difference between the 75th and 25th percentile of the continuous wind exposure measure. Time-invariant controls, interacted by year, include county-level crop suitability, soil characteristics, Dust Bowl erosion measures, and 1935 irrigation intensity. County and state-by-year FE included.

Table A2: Impact of Great Plains Shelterbelt on Jun-Aug crop water availability, 1930 to 1965

	<i>Dependent variable:</i>		
	Palmer Drought Severity Index (PDSI)		
	(1)	(2)	(3)
Wind Exposure:Post 1942	0.994*** (0.162) [0.000]	2.289*** (0.227) [0.000]	1.092*** (0.136) [0.000]
Mean	0.12	0.12	0.12
Std.Dev.	1.83	1.83	1.83
75th-25th Perc. Wind Exp	0.21	0.21	0.21
County FE	Y	Y	Y
State x Year FE	Y	-	Y
Year FE	-	Y	-
Controls x Year	Y	Y	-
Observations	21,528	21,528	24,408

Notes: Standard errors clustered at the county level shown in parentheses; p-values shown in brackets (*p<0.1; **p<0.05; ***p<0.01). Table shows results for estimating Equation 1 for 678 counties, with centroids within 300km of the centroids of Shelterbelt counties. Dependent variables are June - August averages. PDSI measures the departure from the local average of atmospheric moisture. The index ranges from -10 to +10, with lower values signifying stronger drought conditions. Main independent variable is wind exposure (w_i), which measures approximate exposure to winds from afforested areas, interacted by a post-treatment dummy. “75th-25th Perc Wind Exp” shows the difference between the 75th and 25th percentile of the continuous wind exposure measure. Time-invariant controls, interacted by year, include county-level crop suitability, soil characteristics, Dust Bowl erosion measures, and 1935 irrigation intensity. County and state-by-year FE included.

Table A3: Impact of Great Plains Shelterbelt on Jun-Aug county climate, 1930 to 1965
 (Excluding 1936-1942)

	<i>Dependent variable:</i>			
	Precipitation (cm)	Mean Temp (C)	Max Temp (C)	Degree Days (29C)
	(1)	(2)	(3)	(4)
Wind Exposure:Post 1942	0.543*** (0.201) [0.008]	-0.523*** (0.075) [0.000]	-0.811*** (0.108) [0.000]	-9.194*** (1.061) [0.000]
Mean	8.39	23.68	30.87	28.80
Std.Dev.	3.49	3.04	3.17	22.46
75th-25th Perc. Wind Exp	0.21	0.21	0.21	0.21
Observations	21,528	21,528	21,528	21,528

Notes: Standard errors clustered at the county level shown in parentheses; p-values shown in brackets (*p<0.1; **p<0.05; ***p<0.01). Table shows results for estimating Equation 1 for 678 counties, with centroids within 300km of the centroids of Shelterbelt counties. Dependent variables are June - August averages. Main independent variable is wind exposure (w_i), which measures approximate exposure to winds from afforested areas, interacted by a post-treatment dummy. “75th-25th Perc Wind Exp” shows the difference between the 75th and 25th percentile of the continuous wind exposure measure. Time-invariant controls, interacted by year, include county-level crop suitability, soil characteristics, Dust Bowl erosion measures, and 1935 irrigation intensity. County and state-by-year FE included. Separate variable included (not shown) for Wind Exposure:Treat, where Treat is set to 1 for 1936-1942.

Table A4: Impact of Great Plains Shelterbelt on Jun-Aug county climate, 1930 to 1965
 (Excluding 1934, 1936, and 1939)

	<i>Dependent variable:</i>			
	Precipitation (cm)	Mean Temp (C)	Max Temp (C)	Degree Days (29C)
	(1)	(2)	(3)	(4)
Wind Exposure:Post 1942	1.088*** (0.205) [0.000]	-0.480*** (0.064) [0.000]	-0.790*** (0.093) [0.000]	-8.794*** (0.876) [0.000]
Mean	8.39	23.68	30.87	28.80
Std.Dev.	3.49	3.04	3.17	22.46
75th-25th Perc. Wind Exp	0.21	0.21	0.21	0.21
Observations	21,528	21,528	21,528	21,528

Notes: Standard errors clustered at the county level shown in parentheses; p-values shown in brackets (*p<0.1; **p<0.05; ***p<0.01). Table shows results for estimating Equation 1 for 678 counties, with centroids within 300km of the centroids of Shelterbelt counties. Dependent variables are June - August averages. Main independent variable is wind exposure (w_i), which measures approximate exposure to winds from afforested areas, interacted by a post-treatment dummy. “75th-25th Perc Wind Exp” shows the difference between the 75th and 25th percentile of the continuous wind exposure measure. Time-invariant controls, interacted by year, include county-level crop suitability, soil characteristics, Dust Bowl erosion measures, and 1935 irrigation intensity. County and state-by-year FE included. Separate variable included (not shown) for Wind Exposure:Peak, where Peak is set to 1 for 1934, 1936, and 1939.

Table A5: Weather-yield relationship in Great Plains, 1945-1964

<i>Dependent variable:</i>	
Log Yields	
	(1)
Degree Days 10C	0.001 (0.001) [0.333]
Degree Days 29C	-0.013*** (0.003) [0.000]
Degree Days 39C	-0.081*** (0.025) [0.002]
Precipitation	0.006 (0.014) [0.684]
Precipitation ²	-0.001* (0.001) [0.098]
Sample	Wind Exposure <0.01
Time	Post-1942
Obs.	718

Notes: Standard errors clustered at the county level shown in parentheses; p-values shown in brackets (*p<0.1; **p<0.05; ***p<0.01.) Table shows results for estimating Equation 7. Dependent variable (log corn yields) are from USDA 5-year agricultural census (5 censuses between 1945 and 1964).

Table A6: Impact of Great Plains Shelterbelt on Jun-Aug county climate, 1930 to 1965

	<i>Dependent variable:</i>				
	Precipitation (cm)	Mean Temp (C)	Max Temp (C)	Degree Days (29C)	Wind Exposure
	(1)	(2)	(3)	(4)	(5)
Wind Exposure:Post 1942	1.087*** (0.290) [0.000]	-0.756*** (0.059) [0.000]	-0.953*** (0.086) [0.000]	-10.045*** (0.779) [0.000]	
Wind Exposure IV					0.559*** (0.037) [0.000]
Mean	8.39	23.68	30.87	28.8	-
Std.Dev.	3.49	3.04	3.17	22.46	-
75th-25th Perc. Wind Exp	0.21	0.21	0.21	0.21	-
Observations	21,528	21,528	21,528	21,528	598
F-Stat	-	-	-	-	94.46***

Notes: Standard errors clustered at the county level shown in parentheses; p-values shown in brackets (*p<0.1; **p<0.05; ***p<0.01). Table shows results for estimating Equation 3 for 678 counties, with centroids within 300km of the centroids of Shelterbelt counties. Dependent variables are June - August averages. Main independent variable is wind exposure (w_i), which measures approximate exposure to winds from afforested areas, interacted by a post-treatment dummy. This variable is instrumented by the planned wind exposure measure, which reconstructs the wind exposure measure based on the planned 100-mile wide Shelterbelt zone. First stage is shown in Column (5). “75th-25th Perc Wind Exp” shows the difference between the 75th and 25th percentile of the continuous wind exposure measure. Time-invariant controls, interacted by year, include county-level crop suitability, soil characteristics, Dust Bowl erosion measures, and 1935 irrigation intensity. County and state-by-year FE included.

Table A7: Impact of Great Plains Shelterbelt on corn production, area, and yields, using USDA 5-year agricultural census data, 1930 to 1964

	<i>Dependent variable:</i>			
	Log Production	Log Area	Log Yields	Wind Exposure
	(1)	(2)	(3)	(4)
Wind Exposure:Post 1942	3.132*** (0.530) [0.000]	2.163*** (0.474) [0.000]	0.969*** (0.180) [0.000]	
Wind Exposure Instrument				0.537*** (0.033) [0.000]
75th-25th Perc. Wind Exp	0.13	0.13	0.13	
Observations	3,597	3,597	3,597	466
F-Stat	-	-	-	84.06***

Notes: Standard errors clustered at the county level shown in parentheses; p-values shown in brackets (*p<0.1; **p<0.05; ***p<0.01). Table shows results for estimating Equation 3 for 481 counties, with centroids within 300km of the centroids of Shelterbelt counties. Main independent variable is wind exposure (w_i), which measures approximate exposure to winds from afforested areas, interacted by a post-treatment dummy. This variable is instrumented by the planned wind exposure measure, which reconstructs the wind exposure measure based on the planned 100-mile wide Shelterbelt zone. First stage is shown in Column (5). “75th-25th Perc Wind Exp” shows the difference between the 75th and 25th percentile of the continuous wind exposure measure. Time-invariant controls, interacted by year, include county-level crop suitability, soil characteristics, Dust Bowl erosion measures, and 1935 irrigation intensity. County and state-by-year FE included.

Table A8: Synthetic Difference-in-Differences: Impact of Great Plains Shelterbelt on Jun-Aug county climate, 1930 to 1965

	<i>Dependent variable:</i>			
	Precipitation (cm)	Mean Temp (C)	Max Temp (C)	Degree Days (29C)
	(1)	(2)	(3)	(4)
Shelterbelt:Post 1942	0.646*** (0.065) [0.000]	-0.134*** (0.032) [0.000]	-0.213*** (0.045) [0.000]	-3.299*** (0.340) [0.000]
Downwind Neighbor:Post 1942	1.139*** (0.058) [0.000]	-0.127*** (0.0529) [0.000]	-0.207*** (0.038) [0.000]	-3.882*** (0.277) [0.000]
Other Neighbor:Post 1942	0.426*** (0.093) [0.000]	-0.014 (0.028) [0.632]	-0.027 (0.040) [0.512]	-0.256 (0.316) [0.426]

Notes: Standard errors shown in parentheses and calculated using the “jackknife” standard error estimator described in Section IV of Arkhangelsky et al. (2021); p-values shown in brackets (*p<0.1; **p<0.05; ***p<0.01). Table shows results for estimating Equation 9. Dependent variables are June - August averages. Main independent variables are Shelterbelt treatment groups shown in Figure 6.

Table A9: Synthetic Difference-in-Differences: Impact of Great Plains Shelterbelt on corn yields, 1930 to 1965

	<i>Dependent variable:</i>	
	Log Yield (bu/ac)	
	(1)	(2)
Shelterbelt:Post 1942	0.089** (0.037) [0.037]	0.197*** (0.036) [0.000]
Downwind Neighbor:Post 1942	0.170*** (0.035) [0.000]	0.218*** (0.034) [0.000]
Other Neighbor:Post 1942	0.100*** (0.024) [0.000]	0.034 (0.038) [0.381]
Data Source	Census	Survey

Notes: Standard errors shown in parentheses and calculated using the “jackknife” standard error estimator described in Section IV of Arkhangelsky et al. (2021); p-values shown in brackets (*p<0.1; **p<0.05; ***p<0.01). Table shows results for estimating Equation 9. Main independent variables are Shelterbelt treatment groups shown in Figure 6.

Table A10: Irrigation in the Great Plains, 1930 to 1965

	<i>Dependent variable:</i>	
	Change in Irrigation (% of County Area)	
	(1)	(2)
Wind Exposure	3.160*	0.652
	(1.754)	(2.021)
	[0.073]	[0.747]
Mean 1935	0.25	0.25
Mean 1964	2.31	2.31
Mean Change	2.06	2.06
75th-25th Perc. Wind Exp	0.21	0.21
Controls	-	Y
Observations	613	598

Notes: Standard errors shown in parentheses; p-values shown in brackets (*p<0.1; **p<0.05; ***p<0.01). Table shows results for estimating a regression where the dependent variable is the change in the percentage of county area that was irrigated between 1935 and 1964. Main independent variable is wind exposure (w_i), which measures approximate exposure to winds from afforested areas, interacted by a post-treatment dummy. “75th-25th Perc Wind Exp” shows the difference between the 75th and 25th percentile of the continuous wind exposure measure. Controls include county-level crop suitability, soil characteristics, Dust Bowl erosion measures, and baseline 1935 irrigation share of county area.

Table A11: Impact of Great Plains Shelterbelt on Jun-Aug county climate, 1930 to 1965

	<i>Dependent variable:</i>			
	Precipitation (cm)	Mean Temp (C)	Max Temp (C)	Degree Days (29C)
	(1)	(2)	(3)	(4)
Wind Exposure:Post 1942	0.814*** (0.237) [0.001]	-0.495*** (0.072) [0.000]	-0.711*** (0.107) [0.000]	-8.064*** (1.145) [0.000]
:Ogallala				
Wind Exposure:Post 1942	0.736*** (0.227) [0.002]	-0.502*** (0.090) [0.000]	-1.049*** (0.127) [0.000]	-10.857*** (1.229) [0.000]
:Outside Ogallala				
Mean	8.39	23.68	30.87	28.80
Std.Dev.	3.49	3.04	3.17	22.46
75th-25th Perc. Wind Exp	0.21	0.21	0.21	0.21
Ogallala Counties	232	232	232	232
Outside Ogallala Counties	446	446	446	446
Observations	21,528	21,528	21,528	21,528

Notes: Standard errors clustered at the county level shown in parentheses; p-values shown in brackets (*p<0.1; **p<0.05; ***p<0.01). Table shows results for estimating Equation 1 for 678 counties, with centroids within 300km of the centroids of Shelterbelt counties. Dependent variables are June - August averages. Main independent variable is wind exposure (w_i), which measures approximate exposure to winds from afforested areas, interacted by a post-treatment dummy. “75th-25th Perc Wind Exp” shows the difference between the 75th and 25th percentile of the continuous wind exposure measure. Ogallala (Outside Ogallala) is a dummy variable set to 1 for counties over (not over) the Ogallala aquifer. Time-invariant controls, interacted by year, include county-level crop suitability, soil characteristics, Dust Bowl erosion measures, and 1935 irrigation intensity. County and state-by-year FE included.

Table A12: Impact of Great Plains Shelterbelt on corn yields, production, and area harvested, using USDA 5-year agricultural census data, 1930 to 1964

	<i>Dependent variable:</i>		
	Log Production	Log Area	Log Yields
	(1)	(2)	(3)
Wind Exposure:Post 1942 :Ogallala	2.792*** (0.632) [0.000]	2.277*** (0.555) [0.000]	0.515*** (0.192) [0.008]
Wind Exposure:Post 1942 :Outside Ogallala	3.151*** (0.549) [0.000]	3.231*** (0.555) [0.000]	-0.080 (0.171) [0.643]
75th-25th Perc. Wind Exp	0.13	0.13	0.13
Ogallala Counties	135	135	135
Outside Ogallala Counties	346	346	346
Observations	3,597	3,597	3,597

Notes: Standard errors clustered at the county level shown in parentheses; p-values shown in brackets (*p<0.1; **p<0.05; ***p<0.01). Table shows results for estimating Equation 1 for 481 counties, with centroids within 300km of the centroids of Shelterbelt counties, dropping directly afforested areas. Dependent variables are from USDA 5-year agricultural census (8 censuses between 1930 and 1964). Main independent variable is wind exposure (w_i), which measures approximate exposure to winds from afforested areas, interacted by a post-treatment dummy. “75th-25th Perc Wind Exp” shows the difference between the 75th and 25th percentile of the continuous wind exposure measure. Ogallala (Outside Ogallala) is a dummy variable set to 1 for counties over (not over) the Ogallala aquifer. Time-invariant controls, interacted by year, include county-level crop suitability, soil characteristics, Dust Bowl erosion measures, and 1935 irrigation intensity. County and state-by-year FE included.

Table A13: Impact of Great Plains Shelterbelt on Jun-Aug county climate, 1910 to 1965

	<i>Dependent variable:</i>			
	Precipitation (cm)	Mean Temp (C)	Max Temp (C)	Degree Days (29C)
	(1)	(2)	(3)	(4)
Wind Exposure:Post 1942	0.181 (0.163) [0.267]	-0.130** (0.057) [0.022]	-0.303*** (0.083) [0.000]	-3.538*** (0.613) [0.000]
Mean	8.39	23.68	30.87	28.80
Std.Dev.	3.49	3.04	3.17	22.46
75th-25th Perc. Wind Exp	0.21	0.21	0.21	0.21
Observations	21,528	21,528	21,528	21,528

Notes: Standard errors clustered at the county level shown in parentheses; p-values shown in brackets (*p<0.1; **p<0.05; ***p<0.01). Table shows results for estimating Equation 1 for 678 counties, with centroids within 300km of the centroids of Shelterbelt counties. Dependent variables are June - August averages. Main independent variable is wind exposure (w_i), which measures approximate exposure to winds from afforested areas, interacted by a post-treatment dummy. “75th-25th Perc Wind Exp” shows the difference between the 75th and 25th percentile of the continuous wind exposure measure. Time-invariant controls, interacted by year, include county-level crop suitability, soil characteristics, Dust Bowl erosion measures, and 1935 irrigation intensity. County and state-by-year FE included.

Table A14: Synthetic Difference-in-Differences: Impact of Great Plains Shelterbelt on Jun-Aug county climate

	<i>Dependent variable:</i>			
	Precipitation (cm)	Mean Temp (C)	Max Temp (C)	Degree Days (29C)
	(1)	(2)	(3)	(4)
<i>Panel A: 1910 - 1965</i>				
Shelterbelt:Post 1942	0.095*	0.027*	-0.007	-0.430***
	(0.057)	(0.015)	(0.025)	(0.165)
	[0.094]	[0.075]	[0.794]	[0.022]
Downwind Neighbor:Post 1942	0.501***	0.025*	-0.063***	-0.478***
	(0.045)	(0.013)	(0.021)	(0.165)
	[0.000]	[0.054]	[0.003]	[0.004]
Other Neighbor:Post 1942	0.366***	0.076***	0.063**	0.820
	(0.061)	(0.014)	(0.024)	(0.208)
	[0.000]	[0.000]	[0.421]	[0.000]
<i>Panel B: 1919 - 1965</i>				
Shelterbelt:Post 1942	0.248***	-0.059***	-0.115***	-1.544***
	(0.071)	(0.018)	(0.028)	(0.209)
	[0.001]	[0.001]	[0.000]	[0.000]
Downwind Neighbor:Post 1942	0.715***	-0.069***	-0.147***	-2.071***
	(0.050)	(0.015)	(0.025)	(0.167)
	[0.000]	[0.000]	[0.000]	[0.000]
Other Neighbor:Post 1942	0.370***	-0.018	0.004	0.020
	(0.070)	(0.017)	(0.028)	(0.246)
	[0.000]	[0.281]	[0.895]	[0.941]

Notes: Standard errors shown in parentheses and calculated using the “jackknife” standard error estimator described in Section IV of Arkhangelsky et al. (2021); p-values shown in brackets (*p<0.1; **p<0.05; ***p<0.01.). Table shows results for estimating Equation 9. Dependent variables are June - August averages. Main independent variables are Shelterbelt treatment groups shown in Figure 6.

Table A15: Impact of Great Plains Shelterbelt on Jun-Aug county climate

	<i>Dependent variable:</i>			
	Precipitation (cm)	Mean Temp (C)	Max Temp (C)	Degree Days (29C)
	(1)	(2)	(3)	(4)
<i>Panel A: 1925-1930 vs. 1960-1965</i>				
Wind Exposure	1.510*** (0.353) [0.000]	-0.322*** (0.090) [0.000]	-0.814*** (0.138) [0.000]	-5.854*** (0.926) [0.000]
<i>Panel B: 1930-1935 vs. 1950-1955</i>				
Wind Exposure	0.060 (0.362) [0.868]	-0.595*** (0.097) [0.000]	-0.937*** (0.144) [0.000]	-10.484*** (1.275) [0.000]
Mean	8.39	23.68	30.87	28.80
Std.Dev.	3.49	3.04	3.17	22.46
75th-25th Perc. Wind Exp	0.21	0.21	0.21	0.21
Observations	598	598	598	598

Notes: Standard errors clustered at the county level shown in parentheses; p-values shown in brackets (*p<0.1; **p<0.05; ***p<0.01). Table shows results for estimating Equation 4 for 598 counties, with centroids within 300km of the centroids of Shelterbelt counties. In Panel A (B), dependent variables are calculated as the difference between 1925-1930 (1930-1935) and 1960-1965 (1950-1955) June - August averages. Main independent variable is wind exposure (w_i), which measures approximate exposure to winds from afforested areas. “75th-25th Perc Wind Exp” shows the difference between the 75th and 25th percentile of the continuous wind exposure measure. Controls include county-level crop suitability, soil characteristics, Dust Bowl erosion measures, and 1935 irrigation intensity. State FE included.

Table A16: Impact of Great Plains Shelterbelt on Jun-Aug station climate, 1930 to 1965

	<i>Dependent variable:</i>			
	Precipitation (cm)	Mean Temp (C)	Max Temp (C)	Degree Days (29C)
	(1)	(2)	(3)	(4)
Afforested Area (1000 ac) : Post-1942	0.306** (0.151) [0.047]	-0.127** (0.055) [0.025]	-0.140* (0.077) [0.077]	-0.030* (0.016) [0.067]
Observations	2,880	1,872	1,872	1,872

Notes: Standard errors clustered at the station level shown in parentheses; p-values shown in brackets (*p<0.1; **p<0.05; ***p<0.01). Table shows results for estimating a version of Equation 1 with a continuous treatment variable for tree planting (from 2019). This treatment variable is equal to the area afforested within a 25km radius of each station. Dependent variables are June - August averages. Station and year FE included.